

Received:
26 October 2017
Revised:
1 February 2018
Accepted:
6 April 2018

Cite as: Nicholas R. Nalli.
Gunshot-wound dynamics
model for John F. Kennedy
assassination.
Heliyon 4 (2018) e00603.
doi: [10.1016/j.heliyon.2018.e00603](https://doi.org/10.1016/j.heliyon.2018.e00603)



Gunshot-wound dynamics model for John F. Kennedy assassination

Nicholas R. Nalli *

I.M. Systems Group, Inc., 5825 University Research Court, College Park, MD 20740, USA

* Corresponding author.

E-mail address: nallin@img.com.

Abstract

U.S. President John F. Kennedy was assassinated while riding in an open motorcade by a sniper in Dallas, Texas on 22 November 1963. A civilian bystander, Mr. Abraham Zapruder, filmed the motorcade with a 8-mm home movie camera as it drove through Dealey Plaza, inadvertently recording an ≈ 8 second sequence of events that included a fatal gunshot wound to the President in the head. The accompanying backward motion of the President's head after impact appeared to support later "conspiracy theories" because it was claimed that this was proof of a shot from the front (in addition to one from behind). In this paper, simple one-dimensional dynamical models are uniquely applied to study in detail the fatal shot and the motion of the President's head observed in the film. Using known parameters from the crime scene, explicit force calculations are carried out for determining the projectile's retardation during tissue passage along with the resulting transfer of momentum and kinetic energy (KE). The computed instantaneous KE transfer within the soft tissue is found to be consistent with the formation of a temporary cavity associated with the observed explosion of the head, and subsequent quantitative examination of this phenomenon reveals two delayed forces at play in the backward motion of the President following impact. It is therefore found that the observed motions of President Kennedy in the film are physically consistent with a high-speed projectile impact from the rear of the motorcade, these resulting from an instantaneous forward impulse force, followed by delayed rearward recoil and neuromuscular forces.

Keywords: Physics, Mechanics

1. Introduction

U.S. President John F. Kennedy was assassinated while riding in an open limousine within a motorcade through the city of Dallas, Texas on Friday, 22 November 1963. President Kennedy had appeared in countless such motorcades routinely during his presidency. The Dallas motorcade had proceeded without incident up until the end of the route when the President was suddenly shot twice by a sniper. Prior to the arrival of the motorcade, a local civilian named Abraham Zapruder had positioned himself on a 4 foot concrete abutment in the green space known as Dealey Plaza with his state-of-the-art Bell & Howell 8-mm “Zoomatic” color home-movie camera to film the President from a perfect elevated vantage point [1, p. 11]. Shortly after he began filming, he was startled to hear a gunshot, and seeing the President raise his arms, he first thought that the President was morbidly play-acting being shot [2, p. 571]. Mr. Zapruder kept filming while another shot rang out, this one fatally wounding the President in the head. Zapruder would thus both inadvertently and fortuitously record the entire ≈ 8 second sequence of tragic events on film.

The film was initially withheld from the public (given the disturbing graphic violent content), but it was utilized as evidence by the U.S. Federal Bureau of Investigation (FBI) as well as a Presidential Commission established by Executive Order by President Lyndon B. Johnson and headed up by Supreme Court Chief Justice Earl Warren (thus informally known as the “Warren Commission”). The bipartisan Warren Commission (or WC for short) was necessitated after the primary (and only) suspect in the crime, a local man named Lee Oswald, was himself murdered two days later by a local vigilante named Jack Ruby. Based on its investigation, the WC would determine in 1964 from the available evidence that Lee Harvey Oswald was the lone assassin, firing three shots from the sixth-floor southeast (SE) window of the Texas School Book Depository (TSBD) building. The Commission considered the question of a conspiracy, but ultimately found no compelling evidence of one [3, p. 374]. Three additional independent U.S. federal government investigations would affirm the WC’s basic findings [4, pp. 369–381], [5, pp. 50–58], along with other non-government investigations. In spite of the overwhelming physical and circumstantial evidence presented in these investigations,¹ conspiracy conjectures have proliferated in the decades since [4, 5, 6], some out of genuine inquiry concerning a plethora of apparent irregularities in the investigation [7] and “oddities” in the Commission’s findings.

Among these oddities were counterintuitive behaviors and anomalies perceived by WC “skeptics” within the now-famous “Zapruder Film.” However, it was not until a bootleg copy of the film was aired on national television (ABC’s *Goodnight*

¹ In fact, more than 50 separate pieces of evidence implicate Lee Oswald [4, pp. 952–969].

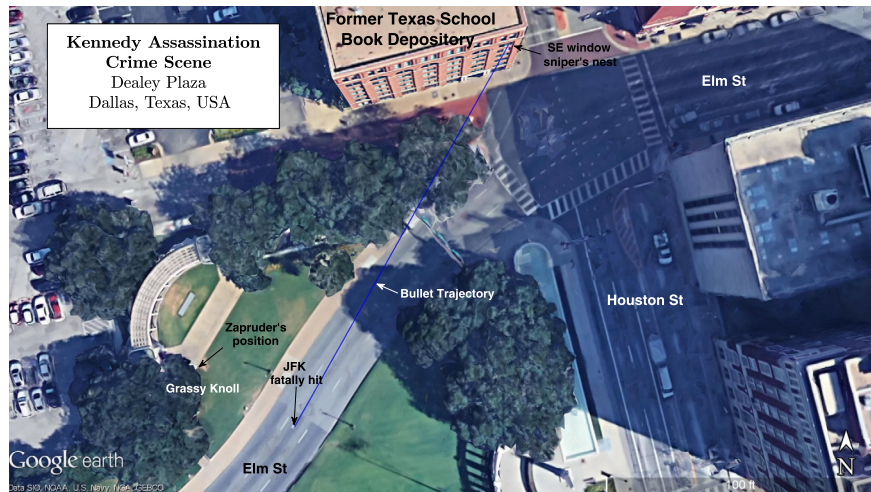


Figure 1. Kennedy assassination crime scene in Dealey Plaza, Dallas, Texas. Shown is the location of cameraman Abraham Zapruder along with the trajectory of the third and fatal shot that killed President Kennedy (blue line) from the Texas School Book Depository (TSBD). The map is oriented with true north pointing toward the top of the page; non-permanent geographic features (e.g., tree canopies, parking lot, road signs, cars, etc.) are contemporary with year 2017 and not as they were in 1963, and the solar shadows are not valid for the historical date and time. Google Earth Pro © map data: Google, SIO, NOAA, U.S. Navy, NSA, GEBCO.

America, hosted by Geraldo Rivera) in March 1975, that a stir was created among the mainstream American public [4, p. 371], [1, pp. 69, 261]. The stir it created is not surprising, given the sequence of events depicted in it, namely the graphic violence, especially the depiction of a fatal wound to the head caused by a high-powered military rifle bullet, something that ordinary citizens would not have had an inkling about in that era. But in particular, the hosts of the program (including Rivera) were adamant about bringing attention to the President’s “back and to the left” movement immediately after being shot, making an unjustified claim that this was “consistent with a shot from the front” (which echoed the assertions of early WC skeptics [8, 9]), in defiance of the other far more definitive evidence that had been made available to the public in the WC Report. Responding to such claims, the illustrious Nobel-prize winning physicist Luis W. Alvarez would shortly thereafter publish his own analysis of the Zapruder Film [10]. Prof. Alvarez examined a number of different questions being posed at the time, including the number of shots (based on jiggle analysis), the shutter speed of the camera, and the President’s reaction to the fatal shot. On the latter question, he concluded that the puzzling backward lurch was the result of a recoil effect (commonly referred to as “the jet effect”); this conclusion has been backed up by subsequent independent experimental studies [11, 12, 13].

In the current paper, the physics surrounding the shot that struck President Kennedy in the head (near-instantly killing him) will be examined in considerably more detail. Figure 1 shows an overview of the Dealey Plaza crime scene (using Google Earth

Pro), including the locations of Mr. Zapruder, the Presidential Limousine (or limo), the sniper's nest, and the trajectory of the shot, which was fired at an approximate distance of ≈ 81 m (266 feet). The weapon purportedly used was an Italian military *Carcano Fucile di Fanteria* (infantry rifle), *Modello 91/38* (Model 1891/1938), manufactured in 1940 at the Royal Arms Factory in Terni, Italy.² This weapon fires ≈ 10.5 g supersonic projectiles with a muzzle speed of 658 m/s that remain highly stable in flight through air. The effect produced by such high-energy projectiles [14, 15] upon collision with a human head is catastrophic as has been characterized through ballistics experiments [12, 16]. In examining this, three separate dynamical phenomena will be considered in Section 2 that explain behaviors observed in the Zapruder Film, namely (1) the initial effect of the forces directly imparted to the target (head) by the projectile (discussed in Section 2.1), followed by (2) the secondary effect of the directional release of explosive energy escaping the skull cavity (discussed in Section 2.2.1), and finally (3) the nervous system reaction to a massive wound to the brain (discussed in Section 2.2.2).

2. Theory/calculation

2.1. Direct impulse effect of projectile-target collision

In the Zapruder Film President Kennedy is seen to react to three separate gunshots, the first missing him and the limo [4, 6, 16, 17], the next two hitting him with increasing accuracy. Further discussion of the first two shots is beyond the scope of this paper other than to note that all three gunshots had associated 1–2 frame anomalous movements, and a outward impulse is observed on the jacket lapel of Texas Governor John Connally (who had accompanied President and Mrs. Kennedy in the motorcade and was collaterally wounded in chest) at the same time the President begins showing signs of being injured [6, 7, 12], but no other discernable impulses are otherwise seen on either of the two men (prior to the third shot).

Figure 2 shows the two Zapruder Film frames that captured the fatal shot, namely Z312 (the moment just before impact) and Z313 (the moment just following impact). In Z313 the catastrophic effect of the energy deposit from a supersonic projectile passing through a human head is clearly evident. However, while it is not immediately noticeable at this scale (and not detectable while viewed in motion at normal speed), a careful comparison between the two frames also reveals that President Kennedy's head *snaps forward* from Z312 to Z313 [9, pp. 87–89], as referenced to the red dashed line labeled *O*. There is nothing new in this

² www.MilitaryFactory.com, Carcano Modello 1891 (M91) Bolt-Action Service Rifle/Carbine (1892); https://www.militaryfactory.com/smallarms/detail.asp?smallarms_id=443.

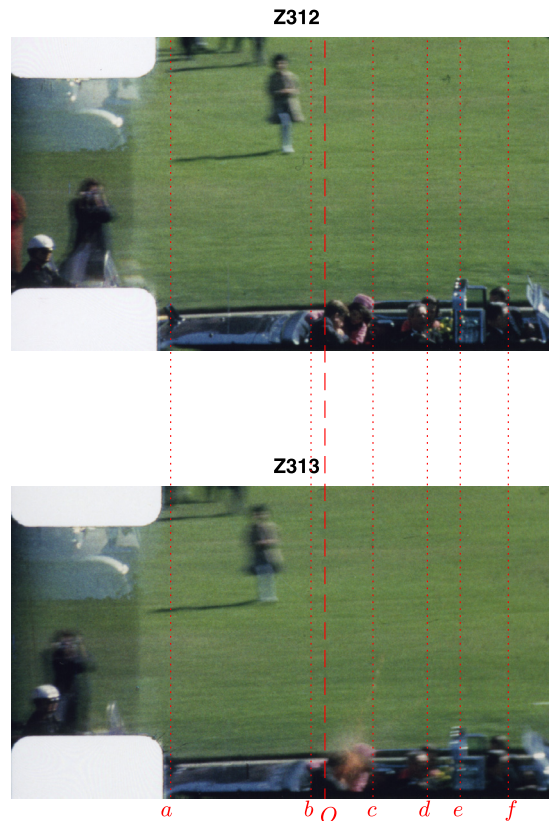


Figure 2. Un-enhanced high-resolution digital copies of Zapruder Film Frames 312 and 313 (Z312 and Z313) showing the high-powered rifle gunshot that fatally wounded President Kennedy. Frame 312 has been horizontally adjusted to correct for tracking error between the two frames. The annotated red line segments demarcate features relevant to the kinematical discussion in the text: dashed line *O* is flush with the back of Kennedy’s head in Z312; lines *a* and *e* are stable limo features (viz., the Secret Service hand grip and chrome window frame, respectively); line *b* is Kennedy’s back; line *c* is Mrs. Kennedy’s hat and hair; line *d* is Governor and Mrs. Connally; and line *f* is the Secret Service agents. Zapruder Film © 1967 (Renewed 1995) The Sixth Floor Museum At Dealey Plaza.

observation—early researchers with access to the still frames first noticed this in the mid-to-late 1960s. Notable among these is author Josiah Thompson, who estimated the position of the President’s head relative to two fixed objects on the rear of the limousine, the results of which are plotted in his book *Six Seconds in Dallas* (1967) [9, p. 91] that will be returned to in Section 2.2. However, for the moment it should be noted that this motion amounts to an anomalous forward impulse on the order of several centimeters over the time interval of one Zapruder frame (≈ 0.055 s) at the moment of impact (an impulse comparable to Connally’s “lapel flap”). It is also crucial to note that this anomalous forward impulse at Z313 is only observed on Kennedy’s head—it is *not* observed on any of the other limo occupants (with reference to dotted lines *c*, *d* and *f*), nor is it even observed on Kennedy’s own torso (line *b*), wherein lies his body’s center-of-mass (CM). This implies that an *isolated real force* acted directly (and solely) upon the President’s head just prior to

Z313; the *only* plausible source for this instantaneous, isolated forcing mechanism is manifestly and unequivocally the projectile impact. Therefore, what follows in Sections 2.1.1–2.1.4 is an examination of the relevant dynamics involved in the direct interaction [18] of a high-speed projectile with a human head.

2.1.1. Model

The interaction of a firearm projectile passing through a human body target constitutes an *inelastic collision*, that is, one where the kinetic energy (KE) of the two-body bullet-target system is not conserved (e.g., in the case of a ballistic pendulum). This concept will be returned to in Section 2.2, but it is noted here that such an interaction nevertheless may not be perfectly inelastic, because the bullet mass passes rapidly through the target rather than merging with it (at least in the case of a high powered military rifle). Because such collisions are neither elastic nor perfectly inelastic, the physical description of the interaction can be more complicated.

Nevertheless, assuming in the case under consideration that the projectile collision occurred near the center of the target (thus not imparting torque), it is possible to consider the interaction in terms of a linear impulse, J_x , which in one dimension for the CM frame is given as [e.g., 19, p. 211]

$$J_x \equiv \int_0^t F_x dt' = M \Delta V_x(t), \quad (1)$$

where t is time, F_x is the scalar force along the x direction of the projectile (bullet) motion, $M \equiv m_p + m_T$ is the combined mass of the system (m_p and m_T being the projectile and target masses, respectively), and ΔV_x is the finite change in velocity of the CM. In this case one may assume that $m_p \ll m_T$ for simplicity; thus $M \approx m_T$ (i.e., the mass of the human head). Equation (1) applies to the bullet passage through an entire head, but this may be broken down into three separate impulses brought on by (1) the skull entrance, (2) passage through the skull cavity (i.e., through the brain), and (3) skull exit. For simplicity, any resistance presented by the hair and scalp is assumed to be of second order and thus negligible [e.g., 20]. Equation (1) is therefore rewritten as

$$M \Delta V_x(t_3) = \underbrace{\int_{t_0}^{t_1} F_1 dt'}_{\text{skull entrance}} + \underbrace{\int_{t_1}^{t_2} F_2 dt'}_{\text{skull cavity (brain)}} + \underbrace{\int_{t_2}^{t_3} F_3 dt'}_{\text{skull exit}}, \quad (2)$$

where t_1 , t_2 , t_3 are the times at which the bullet exits each medium relative to the entrance time at t_0 . From Eq. (2) it is seen that the problem may be treated by

considering separately the collisions of the projectile with a rigid, inelastic skull (both entrance and exit) along with the passage through brain tissue (which may be considered a visco-elastic fluid). It is noted that the projectile was fired from the TSBD on a small downward trajectory ($\approx 16^\circ$ elevation angle) [21, p. 34], and there was a slight downward inclination of Elm Street ($\approx 3^\circ$ or 5% grade) [21, p. 55], with the President's head tilted at a comparable angle slightly down and to his left.

Skull impacts

Attention is first given to the terms involving passage through bone, namely the first and last terms on the right side of Eq. (2). Sturdivan and Bexon [20] derived a model describing the probability of penetration of human skulls by high-speed projectiles (viz., bullets) for military applications based on the empirical observation that such projectiles “punch out” a conical section of skull, a phenomenon known as the beveling or cratering effect [12, 16, 22]. The cratering effect arises from the cross-sectional anatomy of the human skull bone, which consists of inner and outer layers (called “tables” or “laminae”) of hard cortical bone surrounding an internal layer of less-dense “spongy” trabecular (or “cancellous”) bone [20, 23, 24]. As explained by Sturdivan [16, 20], when a high-speed projectile impacts the head and penetrates the skull, it first perforates a hole in the outer table of approximately the same diameter of its own presented area. However, as the bullet breaks through into the inner, less-dense trabecular layer, the area expands roughly in a cone shape until it finally breaks out a wider hole through the inner table. It is this cratering process that assists forensic pathologists in establishing skull entrance or exit wounds [22, 25], thus facilitating the determination of the direction of the bullet's passage relative to the body and the direction of origin of the shot.

Building upon the skull-cratering model described above [20], the impulse force is modeled in the current paper by assuming a perfectly inelastic collision [26, pp. 59–60, 150] between the projectile (Body 1) and the conical section (or “bone plug”) it breaks loose from the skull (Body 2). The interaction of the two bodies during collision according to Newton's Second and Third Laws is given by

$$F_x = -m_1 \ddot{x}_1, \quad \text{projectile (bullet)} \quad (3)$$

$$F_x = m_2 \ddot{x}_2 + F_\sigma, \quad \text{bone plug} \quad (4)$$

where m_1 and m_2 are the masses of the bullet (m_p) and bone plug, respectively, and F_σ denotes the initial force required to break the conical section loose from the skull, noting that Eq. (4) implicitly assumes $|F_\sigma| \leq |F_x| = m_1 \ddot{x}$. F_σ can be estimated from

$$F_\sigma \approx \sigma_u A, \quad (5)$$

where A is the presented area of the projectile and σ_u is the ultimate strength³ of the bone [29, 30, 31], here specifically the cortical table first impacted by the projectile.

Solution of ordinary differential equations (ODEs) (3) and (4) is easily obtained by first recasting them as

$$\begin{aligned} F_x dt &= -m_1 dv_1, \\ (F_x - F_\sigma) dt &= m_2 dv_2, \end{aligned}$$

where $v_1 \equiv \dot{x}_1$, $v_2 \equiv \dot{x}_2$ as usual. Assuming perfect inelasticity, both bodies are deformed and “stick” together immediately after breakage at time t , acquiring a final combined CM velocity⁴ [26, p. 150] of V . Integrating from entrance time $t' = 0$ to t yields

$$\int_0^t F_x dt' = -m_1 \int_{v_1}^V dv'_1 \implies J_x = -m_1 (V - v_1), \quad (6)$$

$$\int_0^t (F_x - F_\sigma) dt' = m_2 \int_{v_2}^V dv'_2 \implies J_x = J_\sigma + m_2 (V - v_2). \quad (7)$$

The impulse caused by the force of the bone breakage, J_σ , is calculated as

$$J_\sigma \equiv F_\sigma \delta t \approx F_\sigma \frac{\delta \mathcal{L}}{v_1}, \quad (8)$$

where $\delta \mathcal{L}$ is the absolute shortening of bone at failure (occurring when the compressive ultimate strength σ_u is surpassed). $\delta \mathcal{L}$ may be estimated from the relative shortening (or engineering strain) at bone failure, \mathcal{E} , defined as [28]

$$\mathcal{E} \equiv \frac{\delta \mathcal{L}}{\mathcal{L}}, \quad (9)$$

where \mathcal{L} is the bone thickness. Values of both σ_u and \mathcal{E} for cortical bone have been variously experimentally determined in the literature which will be returned to in Section 2.1.3.

Combining Eqs. (6) and (7) and solving for V yields the reduced velocity of the bullet (and merged bone plug) after punching through the skull

$$V = \frac{m_1 v_1 + m_2 v_2 - J_\sigma}{m_1 + m_2}. \quad (10)$$

Finally, substituting Eq. (10) into either (6) or (7) and solving for J_x , one arrives at the expression for the impulse imposed by the bullet upon the skull during passage

³ Also variously called the fracture [27] or breaking strengths [28] in the literature.

⁴ In actuality, the “conical section” may break apart into separate pieces [16, p. 196], but it is assumed here that they initially hold-together such that they are uniformly accelerated during the collision.

$$J_x = \frac{m_1 m_2}{m_1 + m_2} (v_1 - v_2) + \frac{m_1}{m_1 + m_2} J_\sigma . \tag{11}$$

Equations (11) and (8) form the basis for calculating the first and third terms of Eq. (2).

The mass of the dislodged bone plug is given by $m_2 = \rho_s \mathcal{V}_c$, where ρ_s is the density of skull bone and \mathcal{V}_c is the volume of the crater, which is modeled to be a conical frustum [20] and thus given by [32, p. 401]

$$\mathcal{V}_c = \pi \delta \mathcal{L} \frac{1}{3} (r_c^2 + r_0^2 + r_0 r_c) , \tag{12}$$

where r_0 and r_c are the radii of the crater entrance and exit holes, respectively, with the latter given by [20]

$$r_c = r_0 + \delta \mathcal{L} \tan(\psi) , \tag{13}$$

ψ being the half-angle of the truncated cone, which is nominally taken to be $\psi \approx 30^\circ$ [20].

Note that if $|F_x| \approx |F_\sigma|$ (i.e., the force of the projectile collision is close to the bone ultimate strength), it is easily shown that (10) and (11) respectively reduce to $V = v_2$ (i.e., the bone plug is not moved beyond its initial speed before impact) and $|J_x| = m_1 (v_1 - v_2) \equiv p_1$, where p_1 is the momentum of the projectile. In this case, the collision would then be a perfectly inelastic collision, and the total incoming momentum of the projectile p_1 would be completely transferred to the skull and head. According to the above model, a projectile impulse J_x will surpass the bone's ultimate strength and thus fracture the bone (although not necessarily perforating it) when $J_x - J_\sigma \geq 0$, that is

$$J_x - J_\sigma = \frac{m_1 m_2}{m_1 + m_2} (v_1 - v_2) - \frac{m_2}{m_1 + m_2} J_\sigma \geq 0 , \tag{14}$$

where J_σ can be estimated from Eq. (8); collision thresholds for bone fracture, given various projectile and bone parameters (i.e., projectile mass or speed, m_1 or v_1 , given target parameters m_2 , v_2 and J_σ), may thus be estimated by finding the corresponding zeros of Eq. (14).

Soft tissue passage (skull cavity)

Using dimensional analysis, Sturdivan [33] derived a drag law for the passage of a spherical projectile through tissue as a combination of an inertial term and a viscous (friction) term

$$F_d = \underbrace{C_i \rho A v^2}_{\text{inertial term}} + \underbrace{C_v \frac{\mu}{b} A v}_{\text{viscous term}} , \tag{15}$$

where F_d is the interaction drag force, C_i is the inertial drag coefficient, C_v is the viscous drag coefficient, μ is the viscosity of tissue (in g/cm^2), b is the thickness of

the viscous boundary layer, ρ is the tissue density, and A is the cross-sectional area presented by the projectile. A more recent drag-law equation valid for a full range of projectile speeds (0–2000 m/s) has been advanced by Peters [34] and features a tissue-strength term in place of a viscous term

$$F_d = \overbrace{\frac{1}{2} C_d(v) \rho A v^2}^{\text{inertial term}} + \overbrace{C_d(v) AR}^{\text{tissue damage term}}, \quad (16)$$

where $C_d(v)$ is a velocity-dependent drag coefficient and R is the “rupture modulus” of the target medium defined as

$$R \equiv \frac{1}{2} \rho \sqrt{v U^3},$$

where U is the “characteristic velocity” of the tissue in question defined by [34]

$$U \equiv U_6 \left(\frac{d}{d_6} \right)^{-\frac{1}{3}},$$

subscripts “6” denoting reference values obtained for a projectile diameter of 6 mm (thus, $d_6 \equiv 0.6$ cm). The tissue-strength term in Eq. (16) becomes more important for lower projectile speeds v [16, 34].

Applying Newton’s Second Law, and assuming A , C_i , C_v , μ and b are constants, Eq. (15) has the solution [33, 35]

$$v(\delta x) = \left(v_0 + \frac{C_v \mu}{b C_i \rho} \right) \exp \left(-C_i A \frac{\rho}{m} \delta x \right) - \frac{C_v \mu}{b C_i \rho}, \quad (17)$$

where v_0 is the initial velocity and δx is the tissue penetration depth. Similarly, for Eq. (16), given projectile impact speeds below 0.7 times the speed of sound in the target medium (i.e., $v \lesssim 1100$ m/s, this being the case for the Carcano bullet), C_d is taken to be constant and (16) is solved as [34]

$$v(\delta x) = v_0 \sqrt{\left[1 + \left(a \frac{U}{v_0} \right)^2 \right] \exp \left(-C_r A \frac{\rho}{m} \delta x \right) - \left(a \frac{U}{v_0} \right)^2}, \quad (18)$$

where C_r is a “reference drag coefficient” and a is a projectile nose-shape parameter that ranges between ≈ 1.2 – 1.9 .

Equations (17) and (18) were both obtained assuming a constant presented area A over the projectile’s trajectory through the medium, δx . However, it is known in practice that a high-speed projectile will undergo deformation from collisions with bone [14, 16, 36, 37, 38], as well as during subsequent passage through soft tissue [16, 38]. This was certainly the case for the Kennedy assassination, as evidenced by the badly deformed bullet fragments recovered from the limousine and autopsy, and will be addressed further in Section 2.1.3.

2.1.2. Projectile retardation in air

For the bullet velocity at impact, v_1 , the retardation of the projectile through the intervening atmosphere must be taken into account. For simplicity this may be taken to be the experimentally measured mean value $v_1 \approx 557$ m/s (55,700 cm/s) [16]. However, to corroborate the measured value, and to facilitate application of the model to an arbitrary source (sniper) location and projectile, the theoretical modeling study in this paper is extended here to include calculations accounting for the projectile passage through the ambient atmosphere of the crime scene.

The bullet impact velocity at the target location may be estimated theoretically by accounting for aerodynamic drag. The one-dimensional aerodynamic drag force is given by [e.g., 16, 19]

$$F_d = \frac{1}{2} C_d A \rho_a v^2, \quad (19)$$

where $v \equiv \dot{x}$ is the speed of the projectile, A is the presented area of the projectile, ρ_a is the mean density of the ambient air, and C_d is the aerodynamic drag coefficient. The equation of motion for the projectile may thus be written as

$$\frac{1}{2} C_d A \rho_a v^2 = -m\dot{v}, \quad (20)$$

where m is the projectile mass. Assuming C_d , A and ρ_a are constants along the projectile path, ODE (20) is easily solved for v as a function of distance traveled, x , by separating variables and integrating

$$\begin{aligned} \frac{1}{2} C_d A \rho_a \int_0^x dx' &= -m \int_{v_0}^v \frac{1}{v'} dv' \\ \implies v(x) &= v_0 \exp\left(-\frac{1}{2} C_d A \frac{\rho_a}{m} x\right), \end{aligned} \quad (21)$$

where v_0 is the initial speed of the projectile at $x = 0$, in this case the Carcano bullet muzzle velocity.

Values for the crime scene parameters may be found in the literature [16, p. 267], namely $x = 81$ m (8100 cm), and for the Carcano rifle bullet (used in the assassination), $v_0 \approx 658$ m/s (65,800 cm/s) and $m \approx 10.5$ g. Although C_d varies with the Mach and Reynolds numbers (Ma and Re, respectively) [16, 39, 40], for the projectile shape (assumed to be spherical) and speed (658 m/s) under consideration, $Ma \approx 1.9 \wedge Re \approx 2.9 \times 10^5$, and thus $C_d \approx 1.0$ [16, 39].

Although the influence of departures of the ambient atmospheric temperature, humidity and wind from a mean state are small [41], the projectile's KE is proportional to the square of its speed. Thus, given the availability of atmospheric surface data, the ambient air density, ρ_a , may be explicitly calculated from the formula [42, p. 52]

Table 1. NOAA Meteorological Surface Observations, Dallas Love Field, 22 November 1963.

Source: NOAA/NESDIS/NCDC [45].

Time (CST)	p (hPa)	T (°C)	T_d (°C)	q (g/kg) [†]	Wind	
					speed, u (m/s)	direction [‡] , ϕ
12:00	1011.5	17.2	10.6	7.9	6.7	248°
13:00	1010.5	19.4	6.1	5.8	8.8	293°

[†] Water vapor mass mixing ratio q is computed from the observed p and T_d values using the formula $q = 622 e/p$, where e is the water vapor pressure, which may be calculated from T_d using published parametric formulas [44].

[‡] In meteorological convention, wind directions are measured clockwise from true north; thus, 0°, 90°, 180° and 270° represent winds from the north, east, south and west, respectively.

$$\rho_a = \frac{p}{R_d T_v}, \quad (22)$$

where R_d is the gas constant for dry air, p is the atmospheric pressure (conventionally reported in hPa), and T_v is the *virtual temperature*, defined as the dry air equivalent temperature pertaining to the density of moist air at the same pressure [43, p. 7]. T_v is calculated as [42, p. 72]

$$T_v \equiv T(1 + 0.61q),$$

where T is the air temperature (K) and q is the water vapor mass mixing ratio (typically expressed as grams H₂O per kilogram dry air, denoted g/kg), which may be computed from the dew point temperature [e.g., 44]. Hourly meteorological surface observations at Dallas Love Field from the U.S. Weather Bureau (the predecessor of the National Oceanic and Atmospheric Administration, NOAA) were obtained from the NOAA National Environmental Satellite Data and Information Service, National Climatic Data Center [45] and given in Table 1.

Because the surface observations were taken at 12:00 and 13:00 Central Standard Time (CST), the values for 12:30 CST (the precise time of the assassination) are obtained simply by taking the means, yielding $\bar{p} = 1011.0$ hPa, $\bar{T} = 18.3$ °C and $\bar{q} = 6.8$ g/kg. From these values and Eq. (22), the mean air density for Dallas, Texas at 12:30, 22 November 1963, is calculated to be $\rho_a = 0.001204$ g/cm³.

Windspeed and direction were included in Table 1 because they factor into the aerodynamic drag calculations (19) and (21) by altering the bullet velocity relative to the fluid. From these, the mean windspeed and direction are calculated to be $\bar{u} = 7.75$ m/s (775 cm/s) and $\bar{\phi} = 270.5^\circ$, respectively. It can be seen that winds were out of the west, which was obliquely against the direction of the bullet trajectory,⁵ thus

⁵ Although beyond the scope of this paper, it should be noted that the prevailing *westerly* winds that day (with 7–9 m/s sustained wind speeds) would also factor into the dispersal of the spray (i.e., the “splatter pattern”) from President Kennedy’s head wound, whereby a motorcycle police officer to the left-rear (i.e., *due east*) of the limo (who is visible in the Zapruder Film, Figure 2) was hit by some of the splatter, in spite of the fact that the spray’s CM was otherwise dispersed forward and upward.

Table 2. Summary of parameters used in impulse force calculations.

Symbol	Parameter	Value	Source
m_1, m_p	mass of projectile (Carcano bullet)	10.5 g	Sturdivan [16, p. 267]
$\overline{r_{HB}}$	average male head-to-body mass ratio	0.061 ± 0.006	Yoganandan et al. [46]
m_{JFK}	mass of President Kennedy	77,100 g	Autopsy Report, CE387 [3, pp. 538–539]
v_0	muzzle speed of Carcano bullet	658 m/s	Sturdivan [16, p. 267]
v_1	speed of Carcano bullet at impact	557 m/s	[16, p. 267] or Eq. (23)
δx_a	path length through air at impact	81 m	Sturdivan [16, p. 267]
δx_H	path length through head	≈ 11 cm	HSCA Appendix VI [21, p. 35]
\mathcal{L}	thickness (path length) of skull bone	0.69 cm	McElhaney et al. [29]
d_0	initial diameter of Carcano bullet	0.67 cm	Sturdivan [16, p. 267]
d_e	effective exit diameter of deformed bullet	2.5–3.0 cm	Autopsy Report, CE387 [3, p. 541]
C_i	inertial drag coefficient (spheres)	0.10	Sturdivan [35]
$C_v \mu/b$	combined empirical constant	≈ 3000	Sturdivan [35]
a	bullet nose-shape parameter (spheres or hemisphere-cylinders)	1.8	Peters [34]
C_r	reference drag coefficient (spheres or hemisphere-cylinders)	0.33	Peters [34]
U_6	reference characteristic velocity (fresh swine liver brain proxy)	87 m/s	Peters [34]
ρ_t	density of brain (soft) tissue	1.04 g/cm^3	Barber et al. [47, p. 85]
ρ_s	density of moistened skull	1.34 g/cm^3	Cammarata et al. [24]
σ_u	ultimate strength of cortical bone (high strain-rate, transverse compression)	$\approx 393 \times 10^7 \frac{\text{dyn}}{\text{cm}^2}$	Keaveny et al. [31]
\mathcal{E}	relative shortening (engineering strain)	$\approx 1\%$	Keaveny et al. [31]
f_z	Zapruder camera shutter frequency	18.3 s^{-1}	WC Report [3, p. 97]

increasing the relative speed and drag. Thus, taking into account the mean headwind, the relative speed of the bullet through the fluid (air) may be estimated as $v'_0 = v_0 + \bar{u} \cos(\delta\phi)$, where $\delta\phi$ is the relative azimuth angle of the wind direction with respect to the bullet trajectory, which can be visually estimated from Figure 1 to be $\delta\phi \approx 60^\circ$. Substituting into Eq. (21) and subtracting the relative wind leaves the reduced bullet speed relative to the ground at impact

$$v(x) = v'_0 \exp\left(-\frac{1}{2} C_d A \frac{\rho_a}{m} x\right) - \bar{u} \cos(\delta\phi), \quad (23)$$

which is calculated to be $v(x) \approx 558 \text{ m/s}$ (55,800 cm/s), this independently being within 0.2% of the mean measured value of 557 m/s (55,700 cm/s) used for impulse calculations in Section 2.1.3.

2.1.3. Calculation

The known parameters from the assassination crime scene may now be applied to the equations derived above. Throughout this paper centimeter-gram-second (CGS) units are used unless otherwise noted. Table 2 summarizes the values used for the parameters (along with their sources) for performing impulse force calculations.

For the skull passage Eqs. (10) and (11), values are required for v_1 (bullet velocity at impact), v_2 (target velocity at impact), m_1 (bullet mass), m_2 (bone plug mass), along with bone impulse force J_σ , which is calculated from Eqs. (5) and (8). The latter calculation requires values for the bullet presented area, A , along with the ultimate strength of skull cortical bone, σ_u , and associated engineering strain, \mathcal{E} .

Values for these parameters may be found in Table 2. For the masses, $m_1 \approx 10.5$ g and m_2 is calculated based upon (12) and (13). For the target velocity, v_2 , the speed of the limousine around the time of impact was estimated by Alvarez [10] to be ≈ 8 mph (≈ 3.6 m/s or 360 cm/s), but there was a rapid deceleration of the limo evident (possibly even braking) [e.g., 5, 6], so it is possible the limo speed was slower than this at the precise moment of impact. Thus, given $v_2 \ll v_1$, one may assume $v_2 \approx 0$ for simplicity. The presented areas of the projectile may be estimated from its diameters at skull entrance and exit. Because the Carcano bullet is extremely stable during normal flight through air, the entrance diameter d_0 is simply the cross-sectional diameter of an unfired bullet, which is known to be 0.67 cm. However, an *effective exit diameter* is assumed based upon the exit wound diameter described in the Autopsy Report found in Warren Commission Exhibit 387 (CE387), namely “a roughly circular wound presumably of exit which exhibits beveling of the outer aspect of the bone and is estimated to measure approximately 2.5 to 3.0 cm in diameter” [3, p. 541]. Although the bullet was broken into at least three fragments [38], it is assumed that the autopsy measurements nevertheless provide an objective best-estimate of the *effective presented area* of the projectile on exit [Sturdivan, L. M., priv. comm.]. To allow for uncertainties [48, pp. 78–79], calculations may be performed for effective exit diameters spanning this range.

The transverse-compression ultimate strength of cortical bone is reported to be 131×10^7 dyn/cm² by Keaveny et al. [31, Table 8.2], although this is based upon quasi-static strain. However, it was also reported that these values can increase by a factor of ≈ 3 for higher-strain rates associated with high-speed trauma such as gunshot wounds [31]; thus, for the case under consideration the ultimate strength will be taken to be $\sigma_u \approx 3 \cdot 131 \times 10^7$ dyn/cm². Finally, the stress-strain curve reported by Keaveny et al. [31] indicates that the engineering strain or relative shortening as defined by Eq. (9) at bone failure (i.e., for stress $> \sigma_u$) is approximately 1% [31, Fig. 8.8].

Soft tissue force calculations may be performed based upon Eqs. (15) and (17) (Sturdivan Model [33]), or (16) and (18) (Peters Model [34]). The total path of the projectile through the brain tissue is taken to be 11 cm, which corresponds to the U.S. House Select Committee on Assassinations (HSCA) description that “the bullet exited at the right coronal suture at a point 11 centimeters forward of the entry wound” [21, p. 35]. This suggests that the bullet path was slightly shorter than the diameter of the head wound, which was described by the autopsy as “a defect which measures approximately 13 cm in greatest diameter” [3, 22, 25]; for a thorough

Finite-Difference Layer Drag Force Calculations

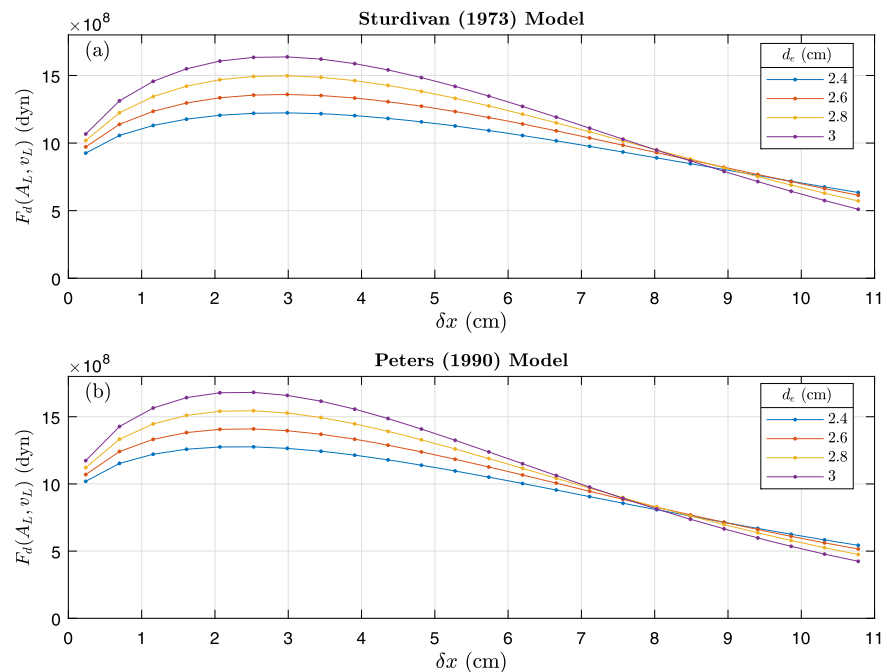


Figure 3. Finite-difference layer drag force computations for deforming (half-parabolic growth) spherical projectile passage through visco-elastic soft tissue (i.e., brain tissue): (a) Eq. (15) (Sturdivan Model), and (b) Eq. (16) (Peters Model). The different colored lines correspond to different effective exit wound diameters, d_e , spanning the range described in the Autopsy Report.

description of the head wound, the reader is referred to Lattimer et al. [12]. It is noted that the massive “defect” was not the “exit wound” of the bullet (as is commonly misunderstood), but rather corresponded roughly to the area where the maximum explosive energy was deposited by the bullet during its passage [16, p. 171] (more on this in §2.2). As mentioned previously, the equations for velocity retardation assume a constant presented area A , and the force equations are dependent upon both A and v . To account for the change in A and v from bullet deformation during passage, a finite-difference approximation is utilized whereby the tissue is broken into finite layers of thickness δx_L and the computation is iterated through the layers. For simplicity, layers are defined with thickness $\delta x_L \approx 0.46$ cm and boundaries thus located at $l = 0, 0.46, 0.92, \dots, 11.0$ cm, yielding $n_l = 25$ boundaries and $n_L = 24$ layers. Given that most of the bullet deformation occurs initially before rapidly diminishing with decreasing velocity [16, p. 171], a simple elliptical growth curve is used to model a continuous increase of A_L from $A_0 = \pi r_c^2$ (r_c being the inner radius of the bone plug computed from Eq. (13)) to $A_e = \pi \cdot (d_e/2)^2$. Then given A_L and v_L , the drag force through the layers $F_d(A_L, v_L)$ may be calculated using either (15) or (16); Figure 3 shows the results for the range of assumed projectile effective exit diameters d_e . Here it is seen that both models yield very comparable results for

the case under consideration, both in terms of magnitude and in variation, thereby providing confidence in their application in this work.

The integrated drag-force impulse is calculated via the finite-difference approximation as

$$J_{xd} = \sum_{L=1}^{n_L} F_d(A_L, v_L) \frac{\delta x_L}{v_L}. \quad (24)$$

Equation (24) forms the basis for calculating the second term of Eq. (2). Note again that the tissue drag force equations were derived assuming spheres [33, 34], so a spherical projectile is also implicitly assumed here. This approximation conveniently eliminates the need to specify the 2-axis orientation of the bullet during passage (e.g., yawing or tumbling). It is recognized that the projectile is assumed to deform and fragment after the initial collision with the skull (which breaches the copper jacket) [12, 38] to the extent that tumbling may be ignored [14], and a primary effect of tumbling is simply to increase the presented area of the projectile [49] which is already accounted for in the finite-difference model Eq. (24).

Figures 4a and 4b show the resulting projectile impulse forces and speed as a function of path length through the head δx , respectively; Figure 4c shows the associated change in projectile KE during passage through the soft tissue (brain) layers calculated as $\Delta K_{L+1} = K_{L+1} - K_L$, where $K_L = \frac{1}{2} m_1 v_L^2$. In Figure 4a one can see the relatively large impulses caused by the entrance and exit impacts on the skull ($J_x \approx 45,000$ and $82,000$ – $93,000$ dyn · s, respectively), the latter encapsulating the range of effective d_e (which are larger due to the projectile deformation during passage). However, the integrated impulse created by drag over the path through the soft tissue, $J_{xd} \approx 280,000$ – $370,000$ dyn · s, is approximately 2–3 times the combined impulses created by the skull entrance and exit. Although the visco-elastic soft tissue presents less resistance than rigid bone, the increased presented area caused by the initial bullet-bone collision and subsequent deformation over a much greater path length yields this greater integrated impulse. Figure 4b shows the reduction of the bullet speed during passage, which translates to the power-of-two loss of KE to the surrounding environment (Figure 4c). Here it is seen that the KE transfer from the projectile to the soft tissue (brain) is maximized before the midpoint, which arises primarily from the increased presented area [16, p. 171] and the associated rate of deceleration from high initial speeds. This large deposit of energy is propagated away from the projectile path via a separated flow field and pressure wave known as *temporary cavitation* [14, 15, 16, 34, 36, 37, 49] (discussed more in Section 2.2).

From the above calculations of J_x (skull entry and exit impulses) and J_{xd} (tissue drag impulse), and given an estimate of the target mass (since $m_T \approx M$), the change in speed ΔV_x of the combined CM at time t_3 (the time of bullet exit) may be readily

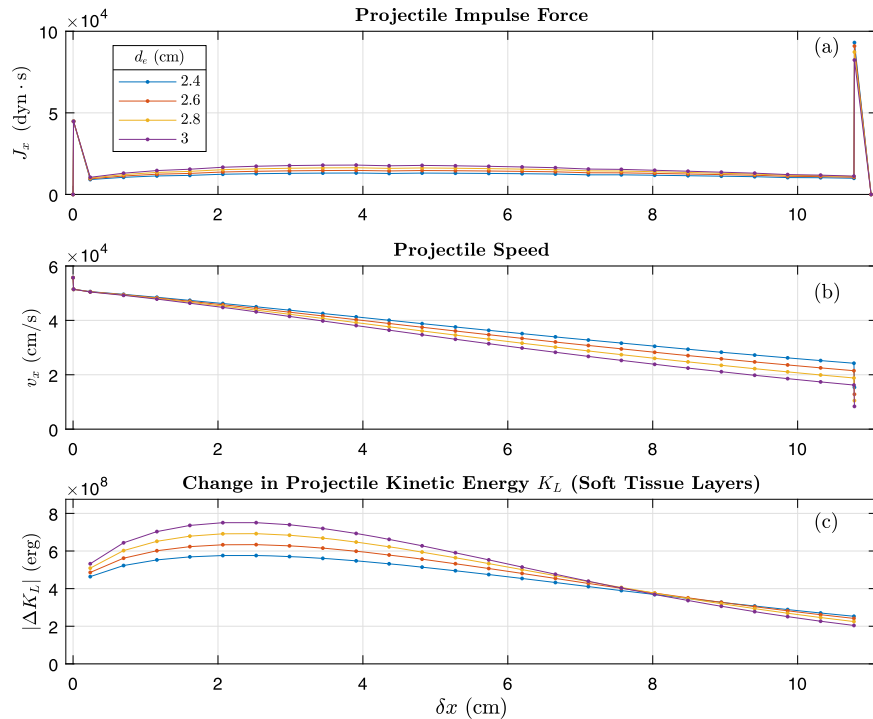


Figure 4. Modeled effects of collision of a deforming, high-speed spherical projectile (i.e., impact speed $v_1 = 55,700$ cm/s) with a human head: (a) computed impulse forces, Eq. (11) and Eq. (24), (b) projectile velocity retardation, Eq. (10) and Eq. (18), and (c) projectile KE loss through soft tissue (brain) layers, $|\Delta K_L|$. The different colored lines correspond to different effective exit wound diameters, d_e , spanning the range described in the Autopsy Report.

calculated. However, to the author’s knowledge, there simply does not exist a precise measurement of the target mass, namely that of President Kennedy’s head (although it may be noted that Kennedy’s hat size is reported to have been $7\frac{3}{8}$,⁶ which is an average size for an adult male). Thus, in this work a best estimate for Kennedy’s head mass is obtained from a tabulation of published anthropometric datasets compiled by Yoganandan et al. [46, Table 18]. Considering only datasets with male-specimen sample sizes $n > 5$, the head-to-total-body mass ratios, $r_{HB} \equiv m_H/m_B$, where m_H and m_B are the head and total-body masses, are found to be remarkably consistent, with the mean here calculated to be $\overline{r_{HB}} = 0.061 \pm 0.006$. The uncertainty estimate (± 0.006) was obtained from the means and standard deviations of the individual datasets tabulated by [46], \overline{m} and σ , using the error propagation formula [48] $u_{HB} = \overline{r_{HB}} \sqrt{(\sigma_H/\overline{m}_H)^2 + (\sigma_B/\overline{m}_B)^2}$. Then, given r_{HB} and an estimate of the body weight, one may then obtain an estimate of the head mass as $m_H \approx m_B r_{HB} \equiv m_T$. Taking President Kennedy’s body weight to have been ≈ 170 lbs as measured from the Autopsy Report [3, pp. 538–539], $m_B = m_{JFK} \approx 77,100$ g, one may arrive at $m_H \approx$

⁶ www.jfklibrary.org/Research/Research-Aids/Ready-Reference/JFK-Fast-Facts.aspx#H.

Table 3. Calculated forward head snap ΔX (inches) caused by Carcano bullet impulse.

Exit Wound Diameter d_e	Moment of impact before Z313 expressed as a fraction of Δt_{ZF}					
	1.0	0.9	0.8	0.7	0.6	0.5
2.4 cm	$+1.9 \pm 0.2$	$+1.7 \pm 0.2$	$+1.5 \pm 0.2$	$+1.4 \pm 0.1$	$+1.2 \pm 0.1$	$+1.0 \pm 0.1$
2.6 cm	$+2.1 \pm 0.2$	$+1.8 \pm 0.2$	$+1.6 \pm 0.2$	$+1.4 \pm 0.2$	$+1.2 \pm 0.1$	$+1.0 \pm 0.1$
2.8 cm	$+2.2 \pm 0.2$	$+1.9 \pm 0.2$	$+1.7 \pm 0.2$	$+1.5 \pm 0.2$	$+1.3 \pm 0.1$	$+1.1 \pm 0.1$
3.0 cm	$+2.3 \pm 0.2$	$+2.0 \pm 0.2$	$+1.8 \pm 0.2$	$+1.6 \pm 0.2$	$+1.4 \pm 0.1$	$+1.1 \pm 0.1$
null exit	$+2.7 \pm 0.3$	$+2.4 \pm 0.3$	$+2.1 \pm 0.2$	$+1.9 \pm 0.2$	$+1.6 \pm 0.2$	$+1.3 \pm 0.1$

The uncertainty estimates correspond to the uncertainty in the estimated target mass. The last row shows values derived from momentum conservation for a total inelastic collision of the projectile with the target (i.e., the bullet does not exit the head), that is $\Delta V_x = v_1 m_1 / M$, where v_1 and m_1 are the speed and mass of the projectile, and M is the combined mass of the two-body system.

4700 ± 500 g. From the estimate for $m_H \approx M$, ΔV_x is then found to be $\approx 90\text{--}105 \pm 10$ cm/s (again, for the range of d_e).

Zero relative motion was assumed before impact, so to obtain an estimate of the total movement of the head from the previous observed position (viz., Z312), ΔX , ΔV_x must be multiplied by the time period over which it moved. Here there is incomplete data, as it is only known that the impact occurred at some point between Z312 and Z313, which spans a total time period of $\Delta t_{ZF} \equiv 1/f_z$, where $f_z \approx 18.3 \text{ s}^{-1}$ is the Zapruder camera shutter frequency, and thus $\Delta t_{ZF} \approx 0.055$ s. From the projectile velocity calculations (Figure 4b), the total time for the bullet passage through the head (i.e., $\delta t_H \equiv t_3 - t_0$ in Eq. (2)) can be estimated by dividing the distances δx by the velocities v_x , then summing them up. From this one obtains $\delta t_H \approx 0.0003$ s, which is more than two orders of magnitudes smaller than Δt_{ZF} . Thus ΔV_x may be taken to be an “instantaneous” step function, implying that one only needs to multiply it by the time difference between the initial impact (sometime between Z312 and Z313) and the shutter opening at Z313 (assuming constant motion). Because the exact moment between frames Z312–Z313 is unknown, one may simply calculate the variation of ΔX over the time interval from the midpoint at steps $\Delta X = \Delta V_x \cdot (0.5 \Delta t_{ZF}, 0.6 \Delta t_{ZF}, \dots, \Delta t_{ZF})$; the results in imperial units (inches) are given in Table 3.

2.1.4. Discussion

Given that the estimated observed head snap observed in the Zapruder Film has been reported to be $\approx 2.2\text{--}2.3$ inches⁷ (≈ 6 cm), these model calculations are found to be of the same general magnitude for the diameters given in the Autopsy Report ($d_e =$

⁷ The 2.3 inch estimate is the value determined by Itek Corporation for the HSCA as reported in Gerald Posner’s book *Case Closed* [6] [pp. 314–315], but the author found a slightly smaller number than this (i.e., $\approx 2.2 \pm 0.2$ in) from digitization of the figure in Josiah Thompson’s book *Six Seconds in Dallas* [9] [p. 91] as is discussed in Section 2.2.2. For consistency with these earlier publications, the imperial units have been retained here.

2.5–3.0 cm). Note that nearly identical results were obtained using the Sturdivan model [33] for the soft-tissue calculations, albeit slightly larger and thus in slightly better agreement, but are not shown in the interest of brevity. Included for reference in Table 3 are calculations assuming a perfectly inelastic collision of the projectile with the target (i.e., the bullet does not exit). The range in calculated exit velocities (Figure 4b, $v_e \approx 80\text{--}150\text{ m/s}$ or $8000\text{--}15,000\text{ cm/s}$) are also reasonable (e.g., these speeds correspond to 2.1–3.8 times as fast as an American major league fastball pitch, which would seem sufficient to inflict damage to the limousine windshield on exit, but not enough to break through it). While Haag [38] experimentally observed the highest exit speed of a fragment to reach 320 m/s, it was noted that other fragments had much lower speeds, and the modeled results in this paper are for the entire combined mass of the projectile plus bone plug fragments.

Note it may also be deduced that the bullet was well airborne at Z312 and the moment of impact probably occurred just after the shutter closed. In fact, the bullet may very well have been just outside or within the camera's field-of-view (FOV) at Z312. This is corroborated by the gruesome image depicted in Z313, where the subsequent explosion of the head cavity is well underway in the wake of the bullet's violent passage (more on this in §2.2.1). The explosion observed in the Zapruder Film and its dynamical effects are explored in more detail below in Section 2.2.

The calculations may have slightly underestimated the observed head snap given that they were based upon a linear impulse imparted to the back-center of the head [16, p. 210]; if the projectile struck somewhat higher than this as proposed by the HSCA [16, p. 191], an additional torque would have imparted additive rotational motion to the top of the head relative to the CM. Additionally, given the downward trajectory of the projectile (and initial inclination of the target), the earth's gravity (which was implicitly neglected) would have imposed a small additional acceleration to the impulse. Another consideration is that the growth of the projectile presented area, A , may have been larger than that estimated using the effective exit diameter—this is quite possible given that the projectile had fragmented (fragments were found in skull cavity during the autopsy) and it would have created secondary missiles [14] from the initial skull collision. Other factors include the assumptions employed in the soft tissue drag formulas, whereby parameters such as the drag coefficient C_d were assumed constant, but more likely varied as the projectile's speed slowed (e.g., the Sturdivan model yielded slightly greater drag). Finally, while uncertainties in parameters were accounted for as much as possible, this could not be done for a handful of them, especially bio-mechanical parameters (e.g., σ_u , U_6 , ρ_t , ρ_s and \mathcal{E}). But all said, the computed magnitudes are found to be physically consistent with (less than) the limiting case of a perfect inelastic collision (i.e., the bullet lodges in the target, transferring all its momentum as in a ballistic pendulum) given in the last

Table 4. Conservation of momentum for bullet and target interaction (cf. Eqs. (25) and (26)).

d_e (cm)	δp_B (g cm s ⁻¹)	δp_T (g cm s ⁻¹)
2.4	-4.234×10^5	$+4.215 \times 10^5$
2.6	-4.501×10^5	$+4.479 \times 10^5$
2.8	-4.746×10^5	$+4.719 \times 10^5$
3.0	-4.969×10^5	$+4.934 \times 10^5$

row of Table 3, and there is otherwise remarkable agreement in magnitude between calculation and observation.

Finally, as a “sanity check” on these calculations, the results should not violate conservation of momentum for the system P , that is

$$\delta P = \delta p_1 + \delta p_2 = 0 \quad (25)$$

$$\Rightarrow -m_1 \delta v_1 = m_2 \delta v_2, \quad (26)$$

where subscripts 1 and 2 refer to projectile and target and it is assumed the masses m_1 and m_2 (given in Table 2) have remained constant throughout the interaction (although the bullet and target fragment into multiple particles, their combined mass nevertheless remains constant). The calculated beginning and ending values for δv_1 are plotted in Figure 4b, and $\delta v_2 \approx \Delta V_x$ (which was used for calculating ΔX in Table 3). The calculated changes in momentum as defined by Eq. (26) are given in Table 4, where agreement between the change in bullet and target momentums are roughly within 0.5–0.7% (target momentum gains slightly less than bullet losses), thereby confirming to first order that the force calculations above have not violated momentum conservation. Additionally, the small deficits in the target momentum gains are consistent with the consideration that the impulse calculations may have slightly underestimated the observed head snap.

2.2. Indirect effects of projectile-target interaction

The phrase “back and to the left” was used in the blockbuster Oliver Stone film *JFK* (1991), whereby the film’s Jim Garrison character (the controversial New Orleans District Attorney) played by Kevin Costner repeats this line as a mantra in a climax courtroom scene while the audience is treated to a loop of the gruesome real-world Zapruder Film on the big screen, interspersed with mysterious gunmen on the Grassy Knoll as “cinematic license.” It is not accidental that this sequence was reserved for the climax of the film: Not only does it innately possess extreme shock value, but it is also presented to the audience as the “smoking gun” (no pun intended) in the argument for a gunman in front of the limousine (paralleling the 1975 *Goodnight America* program), this being the primary physical justification in support of conspiracy conjectures. Figure 5 shows Zapruder Frames Z313–Z316, which

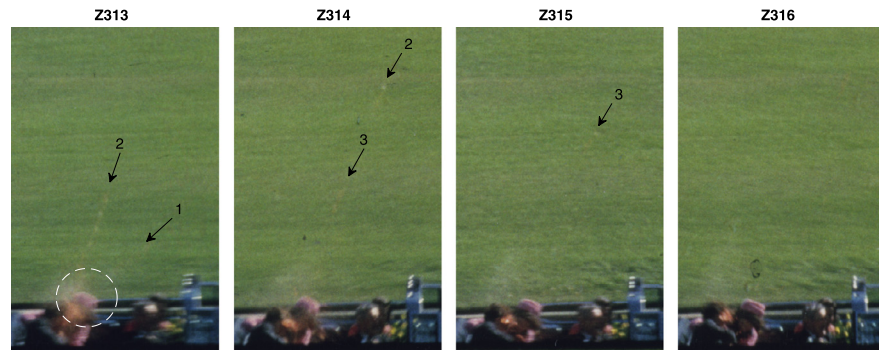


Figure 5. Cropped high-resolution digital Zapruder Film Frames 313–316 showing initial “backward lurch” of President Kennedy along with the distribution of ejected material in the wake of the projectile passage. Frames Z314–Z316 have been adjusted to remove jiggle caused by camera tracking errors of the cameraman. Solid particles (i.e., skull fragments) discussed in the text are annotated with the arrows directed counter to the direction of the particles’ trajectories. Note that the bullet was already long gone by the time the shutter opened at Z313 [50, p. 173]. Zapruder Film © 1967 (Renewed 1995) The Sixth Floor Museum At Dealey Plaza.

capture the “back and to the left” motion exhibited by the President immediately after the bullet impact. Clearly there is a backward movement, but the movement is delayed and slower than the forward impulse discussed above. The impact occurred just following the shutter closure of Z312; this means that the bullet (what was left of it) was long gone by the time of the shutter opening at Z313 [16, 50].

2.2.1. Recoil effect

Alvarez [10] considered this problem based upon simple idealized energy and momentum conservation arguments, along with simple experiments involving tape-wrapped melons as proxies for live human heads; subsequent experiments have repeated Alvarez’s results using more realistic proxies [11, 12, 13]. In this paper, the backward movement is reexamined theoretically in more detail. Like the current author, Prof. Alvarez did not take pleasure in having to delve into this subject matter, but was “convinced that the conclusions... are important” and thus strove to “make the text as free from emotional content as possible.” With that said, Prof. Alvarez realized that “the President’s head did *not* fall back, but was *driven* back by some real force” [emphasis his]. Alvarez estimated that the recoil would be about twice the initial velocity brought about by the collision. He was cautious about the magnitude, but more emphatic about the direction, and modestly deferred the details of the KE transfer mechanism to “someone more knowledgeable in the theory of fluid mechanics.” However, he had already intuited the basic idea, namely that the “conical shape of the interaction zone is the key to the non-negligible efficiency of energy transfer.”

Energy transfer mechanisms

Although the phenomenon of a high-energy projectile passing through a heterogenous body (e.g., a human head composed of hard and soft tissue) falls squarely within the realm of classical Newtonian mechanics, it is nevertheless something not readily observed in everyday experience, and thus not immediately intuitive to the average lay person. Indeed, it is often the case that scientific descriptions of nature are counter-intuitive and can run contrary to common sense [e.g., 51, pp. xi–xii, 1–2]. However, the development of high-speed cameras has gone a long way toward facilitating observation and physical understanding of gunshot wound ballistics.

As pointed out by Alvarez [10], the collision between a high-speed projectile and a human body target is inelastic, with much of the incoming KE going toward “heating” the target. However, the “heating” in question consists primarily in *perturbing* and *deforming* the target. In the case of a Newtonian fluid, the stresses imposed by such perturbations under high Reynolds number conditions (i.e., $Re \approx O(5 \times 10^6)$) leads to the development of a separated flow field and rotational flow features in the form of random eddies (i.e., turbulence) that carry energy and momentum away from their origin. In the case of soft tissue (as opposed to a purely Newtonian fluid such as water), an analogous phenomenon is manifested in what is called temporary cavitation [14, 15, 16, 34, 36, 37, 49], namely the temporary development of a near-vacuum in the wake of the bullet that is rapidly closed via the pressure gradient and elasticity in the tissue [14, 15, 18, 49], resulting in restoring forces that can lead to additional violent undulations before the material fully returns to equilibrium [14, 15].

The temporary cavitation effect leads to an expanding “interaction zone” and can deliver devastating damage to the tissues of a human target, especially less-elastic organs such as the brain [15, 49]. Tragically this is observed in the Zapruder Film. Here the large wound inflicted on the President’s head was not a bullet exit wound, but rather the region of maximum temporary cavitation associated with KE transfer [16, 49]. This KE deposit propagated radially outward in the form of an expanding pressure wave [14, 15] resulting in a rupture and explosion of the skull. Restoring force undulations are also (gruesomely) apparent in the Zapruder Film as brain tissue pulsing and dripping out of the wound in frames Z323–Z330 (not shown here), and Mr. Zapruder himself observed this while filming, as he would later testify to the WC “then I saw his head opened up and the blood and everything came out...” However, all this said, note well that because such explosions are not necessarily the bullet outshoots, the momentum directly carried forward by a given bullet during passage may not be the primary player in a recoil effect.

Model

Thus, in this paper a different method is sought. Rather than attempting to demonstrate or prove the general hypothetical question of whether or not high-speed projectile impacts on head cavities can lead to recoil effects (which Prof. Alvarez and others have demonstrated in the affirmative), one only needs to consider the physics of this particular special case. The objective here is simply to explain the observed behavior in the Zapruder Film, treating it as a case study.

In Z313–Z316 (Figure 5) an expulsion of mass (i.e., the “jet”) is observed resulting from an explosion caused in the wake of a high-speed projectile passage. Although the explosion emanates over a range of angles within a roughly conical cloud, the explosion of mass nevertheless is observed to escape from the single large wound on the right front of the President’s head (described in the Autopsy Report [3, p. 540] and in Lattimer et al. [12]). Note that this is not a universal occurrence—depending on the firearm, bullet, target, entry and exit locations, etc., different “explosions” can result.⁸ But in this case a *directional expulsion of mass* is observed in the Zapruder Film. It is this escape of the explosion from one end of the cavity, but not the other, that creates a directional component to the mass expulsion, and thus a “jet.” In the author’s study of the high resolution digital frames, it was noticed that there were particles that maintained their size and shape over adjacent frames, unlike the rest of the material in the cloud. It was subsequently realized that these were in fact solid skull fragments within a cloud of non-solid tissue, and the author has since learned that previous investigators had already ascertained this [7, 12, 52]. But here it is noted that because these solid particles hold together in flight, they can effectively act as *tracers*, whereby one may estimate the velocity of the ejected mass within the explosion (assuming they travel at the same velocity as the rest of the bulk material).

Shown in Figure 5 are annotations pointing out the locations of 3 such tracer fragments that were sufficiently large enough for the author to identify. Two of these three particles appear in at least two frames, and they appear as double or even quadruple images, this probably resulting from a rapid rotation of the particles [7, 12, 52] with a frequency of 1–2 complete rotations during the course of the shutter exposure. As the skull fragments rotated along their longitudinal axes, they aligned such that the flat sides were perpendicular to the camera FOV. Because they are solid, they hold together during flight, which along with the rotation, facilitates tracking of these pieces as projectiles on the images.

⁸ One may witness this in high-speed camera footage, for example those presented in the 2008 Discovery Channel program “JFK: Inside the Target Car,” as well in other documentaries. High-speed camera frames from a Carcano bullet are also shown in [16, pp. 163–164], where a complete near-isotropic rupture of the skull is evident.

It is thus from these tracer particles that one has sufficient information in hand whereby the classical equation for rocket motion may be applied. To create thrust, the engine of a rocket (or generically, a jet propulsion vehicle) jettisons mass δm with a velocity V_{xe} (typically propellant exhaust via combustion, but any mass ejection would also qualify, including the jettisoning of stages in a multistage rocket) in a direction opposite the direction of travel. This is the result of momentum conservation for the system, involving vehicle and exhaust, for which it can be shown that [e.g., 53, pp. 88–89]

$$\Delta V_x \equiv V_x(t) - V_x(0) = -V_{xe} \ln \left(\frac{M_0}{M_0 - \delta m} \right), \quad (27)$$

where V_{xe} is the velocity of the exhaust in the moving vehicle frame, defined here as positive along $+x$ (left to right relative to the camera FOV), M_0 is the starting total mass of the system (vehicle plus propellant) and δm is the propellant mass. Thus it is seen that the thrust is dependent on both the mass *and* velocity at which the propellant is expelled.

Regarding the current application, while the exact mass of the exhaust “jet” is not known, one may estimate it to be on the order of $20 \pm 10\%$ of the total brain mass.⁹ However, unlike a typical rocket vehicle, the jet under consideration was not constrained along a tube to exit mostly along a single vectorial direction, but rather erupted in a roughly conical cloud over a finite range of directions. Nevertheless, because it originated from a opening on one side of the cavity, the jet (or, perhaps more accurately, “spray”) exhibits a mean direction of motion in the forward-upward-right direction relative to Elm Street [52, p. 63]. The directional momentum for the spray’s CM is $\mathbf{p} = \delta m \mathbf{v}_s$, where $\mathbf{v}_s \equiv \dot{\mathbf{r}}_s$ (the velocity of the exhaust spray), and thus the x -component (defined as positive down Elm Street, counter to the bullet trajectory and left-to-right in the Zapruder frames) is given by

$$p_x = \delta m \dot{r}_s(\theta, \delta\phi) \cos(\theta) \cos(\delta\phi), \quad (28)$$

where θ is the mean relative elevation angle and $\delta\phi$ is the mean relative azimuth angle, measured clockwise from x around the local zenith, z , of the spray CM. Assuming $\delta\phi \approx 0^\circ$, one may then estimate the maximum velocity of the spray’s CM by examining the tracers identified in Figure 5. The x -component of this would then constitute the jet exhaust speed in (27), which from Eq. (28) one then has

$$V_{xe} = \dot{r}_s \cos(\theta). \quad (29)$$

⁹ These values are an estimate based upon autopsy pathologist testimony that “two thirds of the right cerebrum had been blown away” [25] (i.e., about 1/3 of the total cerebrum, which is 90% of the total brain [54], thus 30%), and recognizing that a fraction of this total mass lost occurred well after the “peak explosion” and does not factor into the jet, thus <30%. Alvarez [10] assumed a jet mass of 10% the total weight of the head in his paper, but noted that “the assassination buffs” considered this value to be too high (which may in fact be the case).

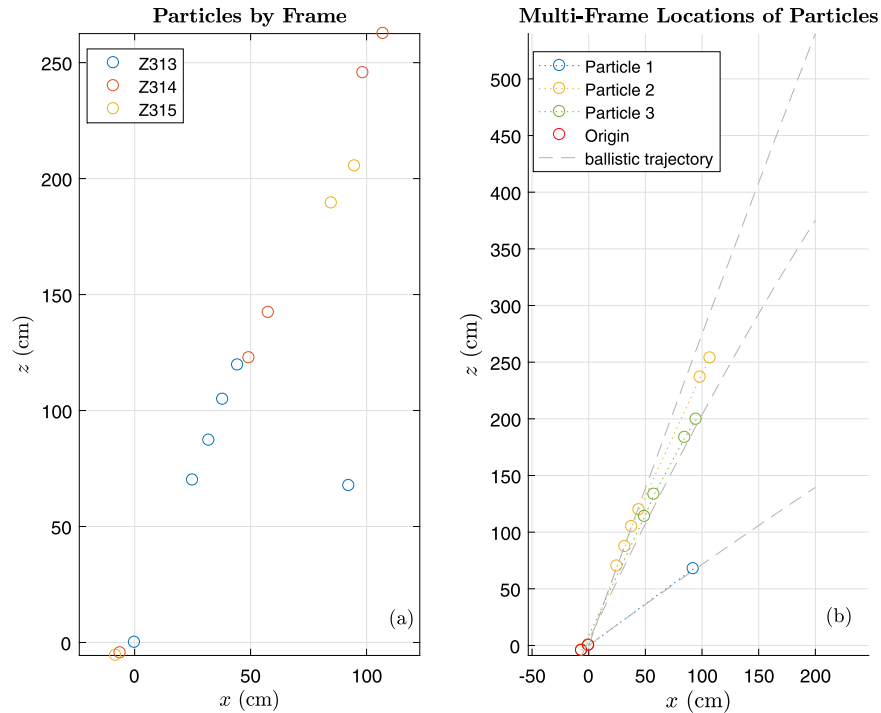


Figure 6. Graphs of the approximate locations of solid particles observed in the Zapruder Film: (a) particle locations by frame indicated by different colored circles, and (b) multi-frame locations of 3 individual particles (distinguished by color), with the approximate “origins” indicated in red circles, and dashed gray lines indicating approximate ballistic trajectories (neglecting air resistance) for the estimated angles and particle speeds.

Using the “head snap” estimate of 2.3 inches, and assuming that the particle positions fall roughly within a plane orthogonal to the camera’s FOV, the author was able to perform a rough conversion of image pixels to centimeters and thus grid the approximate locations of the particles. Shown in Figure 6 are Cartesian plots charting the locations and movement of the particles—the lefthand plot shows the particles for each frame and the righthand plot shows the frame-to-frame motion of individual particles. Particle 1 is not readily visible over two frames and the time interval between impact and Z313 is not perfectly known (as discussed in Section 2.1.3); thus, this particle is not used for estimating the explosion speed, but will be returned to below. However, Particles 2 and 3 span multiple frames, Z313–Z314 and Z314–Z315, respectively, and thus the shutter frequency provides the time interval. From the multi-frame points plotted in Figure 6b, the velocity of the particles may be estimated from two successive frames as $v_p = S/\delta t = S f_z$, where S is the slant path of the particle trajectory computed as $S = \sqrt{\delta x^2 + \delta y^2}$. From this crude approach, speeds for Particles 2 and 3 identified in Figure 6b are estimated as $v_p \approx 3000$ and 1400 cm/s (≈ 67 and 32 mph, respectively). Figure 6b shows estimated ballistic trajectories neglecting air resistance based upon these estimated speeds and trajectory angles, which although not perfectly matched (due to neglecting drag),

nevertheless illustrate that the particles roughly follow ballistic trajectories. The estimate for Particle 2 is smaller than, but reasonably close to, the estimate obtained by the Itek Corporation for the HSCA, which was ≈ 80 mph (≈ 3600 cm/s) [52, p. 62], [7, p. 333]. The slower speed estimates obtained empirically by the author may be attributed to the fact that they were obtained from Z313–Z314 (Particle 2) and Z314–Z315 (Particle 3), whereby air resistance had already damped their speed, and in the case of Particle 3 the explosive KE from the wound had already partially dissipated.

However, these empirical velocity estimates for the spray (or jet) may be theoretically arrived at by revisiting the conservation of energy for the system

$$\delta K_B \equiv K_B(t_1) - K_B(t_2) = Q_B, \tag{30}$$

where δK_B is the KE loss of the bullet during passage through the target (the target here being the brain), Q_B is the energy imparted to the target, and t_1, t_2 are entry and exit times of the bullet as expressed in Eq. (2). The resulting KE of the system of particles comprising the target can be separated into two parts: (1) the KE of individual particles relative to the CM frame, and (2) the KE of the CM relative to an inertial frame. This is expressed as [e.g., 55, pp. 109–110]

$$Q_B = \frac{1}{2} \sum_{i=1}^N m_i \dot{r}_i^2 + \frac{1}{2} M_B \dot{R}_B^2, \tag{31}$$

where M_B is the total brain mass, and \dot{R}_B and \dot{r}_i are velocities of the brain CM and individual particles relative to the CM, respectively. The second term on the right is equivalent to the KE associated with the soft-tissue impulse contributing to the observed forward head-snap (which shall be denoted K_I) and has been calculated in Section 2.1. The first term, on the other hand, is associated with “heating” (viz., inelastic disruption and deformation) of the target, a part of which goes toward the momentum of the spray that erupts from the cavity. If one defines a mean-square speed of the particles (relative to the CM), $\overline{\dot{r}^2}$, Eq. (31) may be simplified as follows

$$\begin{aligned} \overline{\dot{r}^2} &\equiv \frac{\sum_{i=1}^N m_i \dot{r}_i^2}{\sum_{i=1}^N m_i} \implies \frac{1}{2} \sum_{i=1}^N m_i \dot{r}_i^2 = \frac{1}{2} M_B \overline{\dot{r}^2} \\ \implies Q_B &= \frac{1}{2} M_B \overline{\dot{r}^2} + K_I, \end{aligned}$$

which when substituted back into Eq. (30) leaves

$$\dot{r} = \sqrt{\frac{2}{M_B} (\delta K_B - K_I)}. \tag{32}$$

One may thus use Eq. (32) to estimate $\dot{r} \approx \dot{r}_s \equiv v_s$ given values of δK_B and K_I (as calculated in Section 2.1.3), and an estimate of the brain mass, M_B . Although the

autopsy reported the brain mass to be 1500 g, this number will be too small due to the loss of tissue, blood and fluid from the gunshot wound. Given the assumed brain loss for the jet spray of $20 \pm 10\%$ (as discussed in Footnote 9), the living brain mass before wounding is taken to be 40% more than the autopsy-measured value, thus $M_B \approx 2100$ g. From these parameters, the theoretical spray speed v_s is subsequently calculated to be in the range of ≈ 3200 – 3500 cm/s (depending on the assumed exit wound diameter), which are in general agreement with the observed values from the Zapruder Film, thus lending confidence to these estimates. It may also be noted that although these particle exit speeds appear “fast” by everyday experience, they are significantly slower than the projectile depositing the energy; thus the explosion lags the projectile impulse [50, p. 173].

Returning to the application of Eqs. (27) and (29), although one has reasonable ranges for the mass and mean angle of the jet spray, that is $\delta m \approx (0.2 \pm 0.1)M_B$ and $\theta \approx 40$ – 80° , the exact values are not known (the latter estimate is from visual inspection of Z313). As in Section 2.1.3, the recoil *distances* are obtained from the change in velocities calculated from Eq. (27) as $\Delta X_r = \Delta V_x \cdot \Delta t_{ZF}$; for convenience in interpretation of the results, they are given in the head-snap frame, thus the initial motion of the “vehicle” (i.e., the head) is taken to be zero, $V_x(0) = 0$ cm/s. In reality, the head was initially moving at speed $\Delta V_x(t_3)$ from a pre-existing momentum imparted by the impulse from the bullet collision as per Eq. (2), but it is easier to observe the recoil effect without this initial velocity superimposed. To allow for the uncertainties in the parameters δm , θ and V_{xe} , calculations are simply repeated for parameter ranges encompassing realistic values [48, pp. 78–79], with the subsequent results (in inches per Zapruder frame) conveniently summarized as contour plots in Figure 7.

Results and discussion

The first most noticeable feature are the signs of the calculated ΔX_r , these all being negative, which indicates deceleration (acceleration in the negative x -direction). This calculated recoil displacement can be translated to the observed changes of position in the Zapruder Film by re-adding the initial velocity. Because the movements are restricted to finite time intervals (camera shutter speed), one may do this simply by adding the calculated values of ΔX_r to the observed forward head-snap displacement of ≈ 2.3 in (or 2.2 ± 0.2 inches as estimated by the current author from [9]). Thus absolute values of $\Delta X_r \approx 2.0$ – 2.5 inches (5–6 cm) represent “stoppage” of the forward head-snap (i.e., no change in position from Z313 to Z314, whereas $|\Delta X_r| \gtrsim 2.5$ in represents rearward displacement; absolute values smaller than 2.0 in indicate only a “slow-down” of forward momentum. Of course, a small amount of retrograde motion in the President’s head is already seen in Z314; thus, the

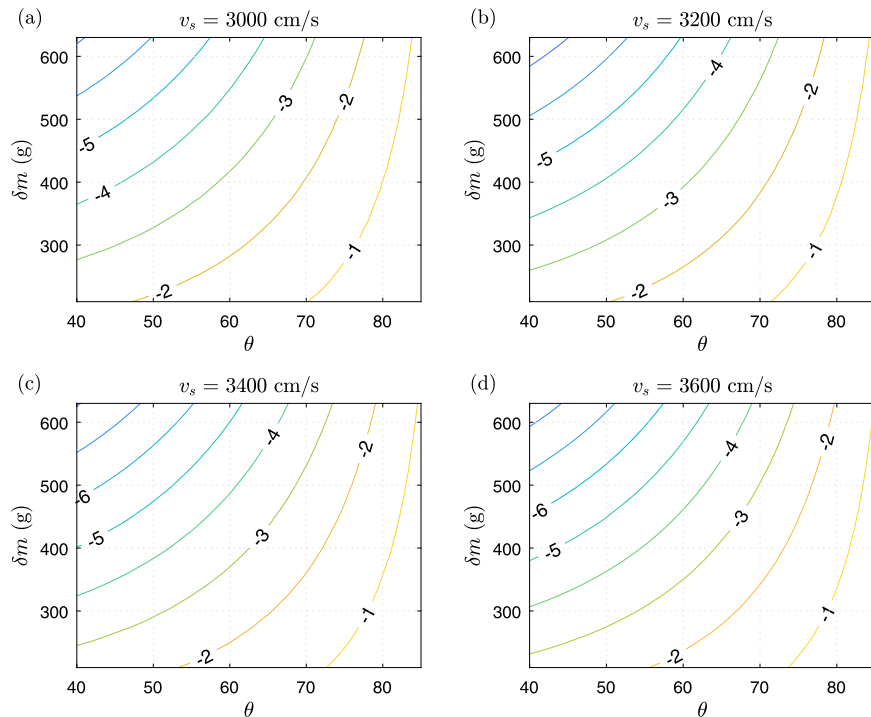


Figure 7. Calculated recoil displacements ΔX_r (inches per Zapruder frame) using Equation (27) for assumed exhaust jet (or “spray”) velocities, v_s : (a) 3000 cm/s, (b) 3200 cm/s, (c) 3400 cm/s, and (d) 3600 cm/s. The abscissa and ordinate of each plot are the assumed mean elevation angles and mass of the spray, θ and δm , respectively. To obtain the actual change in position of the President’s head from Z313 to Z314, these values must be superimposed upon the observed speed of the forward head-snap between Z312 and Z313, namely ≈ 2.0 – 2.5 inches per Zapruder frame.

actual absolute magnitude of the retrograde displacement brought on by the recoil was ≥ 2.3 inches, but only slightly so ($\approx 0.6 \pm 0.3$ in as shall be seen in Section 2.2.2). Thus it is noted that the required magnitude of the recoil displacement between Z313 (during a forward head-snap) and Z314 is $|\Delta X_r| \approx 3$ inches (≈ 2.3 in to counter the existing forward motion, plus an additional ≈ 0.6 in) is of the same order of magnitude of values shown in Figure 7, and well encompassed within the ranges. Generally these results tend to suggest the following: (1) there was an oblique mean elevation angle of the spray (i.e., $\theta \gtrsim 40^\circ$), which is visually the case in the Zapruder Film; and (2) although the total loss of brain mass may have been greater, the mass of the actual spray (or jet) contributing to the recoil was plausibly in the range of $\approx 20\%$ (420 g) as assumed, this being somewhat less than the 10% total-head mass assumed by Alvarez [10]).

Attention may be turned back to Particles 1 and 2 identified in Figures 5 and 6. Given the estimated speeds of the exhaust spray, along with the estimated path lengths S in Z313, one may obtain an independent estimate the actual moment of bullet impact between Z312 and Z313 from $\delta t = S/v_s$; as elsewhere in this paper, this may be

expressed in terms of a fraction of the Zapruder camera shutter speed, Δt_{ZF} , simply by multiplying by the shutter frequency f_z . For the spray speeds shown in Figure 7 (i.e., $v_s = 3000\text{--}3600$ cm/s, the projectile impact before Z313 is estimated to occur a fraction of a shutter cycle, $\zeta \approx 0.7 \pm 0.1$. If one includes an estimate for the time lag of the cavitation pulse (e.g., 0.005–0.01 s) [7, p. 213], then the estimated impact time fraction increases to $\zeta \approx 0.85 \pm 0.15$. These values for impact time agree reasonably with those required for a $\approx 1.5\text{--}2.0$ inch (4–5 cm) head snap from the projectile impulse given in Table 3. Note these values were arrived at through completely independent means, one via the explicit impulse force calculations detailed in Section 2.1, the other via estimation of the exhaust speed of the jet from the head explosion. Finally, from these values, one may estimate the location of the Carcano bullet at Z312 (given its impact speed, v_1) as approximately $v_1 \cdot [(1 - \zeta) \Delta t_{ZF}]$. For the range of ζ , the bullet would thus have been within 12 m of the President at Z312 (or within 9 m when taking into account the cavitation delay); thus it is possible that the bullet was just outside or even within the camera FOV at Z312.

As a final note, all these calculations have treated the head as a ballistic pendulum [10]. In the absence of other forces, the President's head would have ultimately stopped its forward motion simply because of its anchor to the remainder of the body before finally going limp. But even assuming this damping effect was also at play, to re-quote [10], “the President's head did *not fall* back, but was *driven* back by some real force,” and without this real force the President would have simply succumbed to gravity and fallen forward or sideways in the seat; thus damping by itself cannot explain the “rearward lurch.” And even assuming it was at least partially at play, there is still room to accommodate a partial slow-down of the forward head-snap due to a damping effect in the range of calculated recoil magnitudes in Figure 7 (especially for the smaller assumed jet masses and velocities or the larger θ).

Thus, the “laws of physics” (specifically, conservation of energy and momentum) affirm that a recoil effect (or jet effect) is consistent with the specific circumstances of President Kennedy's head wound as observed in the Zapruder Film. The observed recoil was the result of a directional explosion of mass caused by the KE deposit of a high-speed projectile, and this initiated the tragic final backward lurch of the President. But is this the complete story? This question is explored briefly in the next subsection.

2.2.2. Neuromuscular effect

Those familiar with the various details of the Kennedy Assassination may already be aware of another alternative explanation for the “rearward lurch” seen in the Zapruder Film, namely the “neuromuscular reaction” hypothesis [50, p. 174], [6, p. 314]. Admittedly, the author at one time was dubious about this explanation as it

seemed to be speculative without any solid scientific footing. But it turns out there are reasonable physiological arguments that indicate a biological effect was also at play. Neuromuscular spasms are known to result from traumatic brain injury [11], and such reactions have been observed in laboratory experiments on goats as well in military combat [16]. One plausible explanation is a stretching of the spinal cord caused by shear forces arising from the massive agitation of the brain (as discussed in Sections 2.1.3 and 2.2.1). The stretching of the spinal cord can cause minor damage to the nerve cells affecting their ability to hold electrical charge, thereby resulting in a sudden nerve discharge stimulating all the muscles of the body, with the larger and stronger muscles of the torso winning out [16, pp. 164–169]. However, what is particularly relevant to the current analysis is the consideration that a nervous system response to brain trauma resulting in a muscle spasm typically occurs on a delayed time scale [7, pp. 342–343, 369] on the order of tenths of a second [e.g., 16, pp. 169–170, 301–302], which approximately translates to 2–10 Zapruder frames.

So is there any objective quantitative evidence for this hypothesis related to the case under consideration from the dynamics point-of-view of this paper? It turns out there is, and it is again supplied by what is observed in the Zapruder Film itself. Figure 8a is an annotated replication of the figure measuring the position of the President's head x_i for Zapruder frames $i = Z301$ to $Z329$ (skipping $Z318$, presumably due to camera jiggle) relative to the rear seat of the limo that appeared in Thompson's book *Six Seconds in Dallas* [9, p. 91]. The data have been re-plotted by the current author (Figure 8a) based upon digitization of the original image, which was notable for showing both the initial “forward snap” of the President's head from $Z312$ to $Z313$, along with the “rearward lurch” from frames $Z313$ to $Z322$. However, after studying the original figure it was noticed that there appeared to be subtle accelerations and decelerations. Thus, first- and second-order differences have been performed on the original position data points, the results plotted in Figures 8b and 8c, respectively. The first-order differences, $\Delta X / \Delta t_{ZF}$, represent the change in position per Zapruder frame and are indicative of velocity whereas the second-order differences, $\Delta(\Delta X) / (\Delta t_{ZF})^2$, are indicative of acceleration.

From these latter two plots one may more carefully (and quantitatively) observe the kinematics. In Figure 8b the velocity imposed by the impulse stands out as a 1-frame positive spike at $Z313$ of +2.2 in (+5.5 cm) that is immediately followed by an immediate reversal to -0.6 in (-1.6 cm). This backward motion gradually increases to a negative peak of greater magnitude, that eventually succumbs to a sustained forward velocity. The latter forward motion is associated with the President going limp and slumping over, but in the rearward motion one may already discern two distinct peaks. Thus attention is directed to the third plot (Figure 8c) where significant accelerations of the President's head are readily seen, these being indicative of external forces. A number of anomalous accelerations are evident,

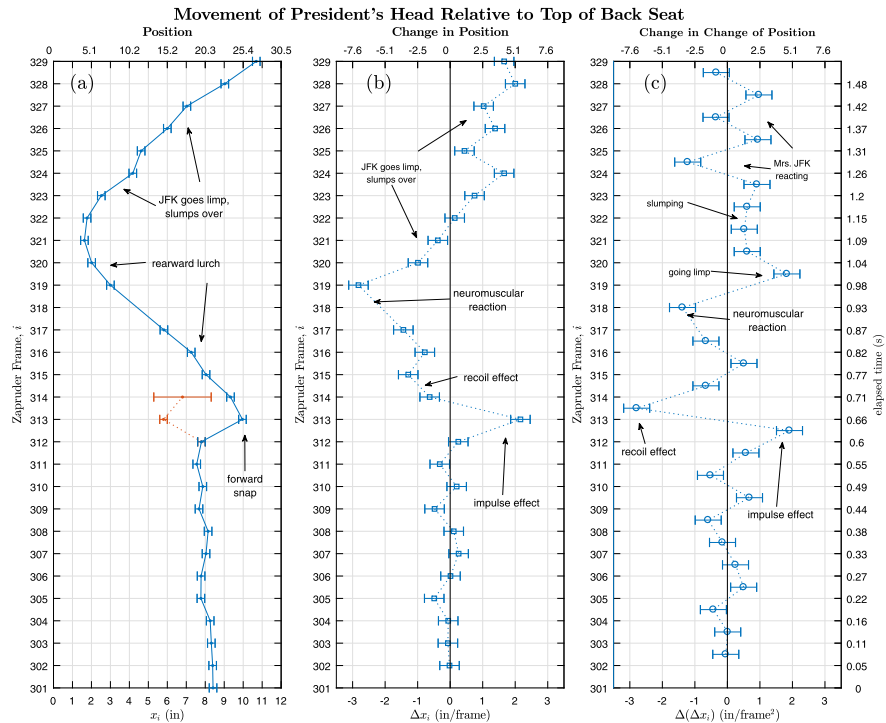


Figure 8. Motion of President Kennedy’s head relative to the rear of the seat of the limousine determined from the Zapruder Film by Kennedy assassination author Josiah Thompson: (a) position of the President’s head relative to the rear seat as originally published by Thompson [9, p. 91], with red data points showing impulse and recoil model-predicted values from a hypothesized frontal shot assuming the same weapon (as discussed elsewhere in the text), (b) first-order change in position calculated as $\Delta x_{i+1} = x_{i+1} - x_i$, where i is the frame number, and (c) second-order change of position calculated as $\Delta(\Delta x_{i+2}) = \Delta x_{i+2} - \Delta x_{i+1}$ (plotted at the midpoints between frames $i+1$ and $i+2$). Error bars denote uncertainty estimates [48] based on those shown in [9, p. 91] (a), and propagated through the first- (b) and second order differences (c). The rightmost y-axis shows approximate elapsed time in seconds, and the top x-axis shows distances in centimeters. Data points are linearly connected by dotted lines in (b) and (c) to assist with pattern recognition, but do not accurately represent non-linear high-speed changes between data points, especially the impulse and recoil spikes. Note that there was no data point at Z318 due to blurring of the frame from camera jiggle.

the first being the initial collision impulse (between Z312 and Z313) followed immediately by the recoil (between Z313 and Z314). Here the absolute magnitude of the recoil force is seen to be about 50% larger than the impulse force, this being required for the deceleration of the forward head-snap and initiating the “rearward lurch.” However, like the impulse acceleration, this initial rearward acceleration lasts only one frame, returning to a near-equilibrium state of near-zero acceleration for one frame before a distinct *second* rearward acceleration is evident, albeit this one slower (increasing over two frames instead of one) and obviously delayed. Therefore it is seen that the so-called “rearward lurch” was in fact caused by *two distinct forces*, not simply one. There is simply no other plausible explanation for the delayed secondary acceleration than that of a neurological muscular response. This statement

is supported by the fact that in the Zapruder Film frames (Figure 5), the initial acceleration (the recoil effect) is observed on the head only (Z313–Z315), whereas the latter acceleration, beginning around Z317 and peaking at Z318 (these being ≈ 5 –6 frames following Z312, which is consistent with a nervous system response), is observed to originate from the President's torso [52, p. 80], [7, pp. 338, 343] (i.e., it is his entire upper body that is seen to be propelled backward relative to the limo seat). The only mechanism that could cause the President's upper torso to torque backward in the seat (but not the other limo occupants) would be a real force directly applied to his upper torso, not his head. A force applied only to the head would simply cause the head CM to pivot on the neck as did the initial projectile impulse at Z313. The only plausible forcing mechanism available to the upper torso as seen in the film would be a contraction of the President's own torso muscles. In discussing this it should be also recognized that President Kennedy wore a lower back brace, so a brief contraction of the lower back muscles would not visibly arch his back. The Zapruder Film thus corroborates that another delayed (5–6 frame) forcing mechanism was at play (in addition to the projectile collision impulse and head cavity recoil), and a neuromuscular spasm is the only physically plausible mechanism known to this author.

2.2.3. *A near-simultaneous shot from the front?*

From reasoning similar to that presented in Section 2.1, many have argued over the intervening decades that the rearward lurch (or “back and to the left” motion) of President Kennedy shortly after the fatal impact at Z313 “proved” an impact from the front [e.g., 7, 8, 9, 56, 57, 58], possibly even as a second near-simultaneous shot [9, pp. 94–95]. Any conclusive proof of a shot from the front would ergo be proof-positive of the existence of a conspiracy. Would a rifle shot from the front explain the rearward lurch?

The short answer to this question is “no” because there was no cratered exit wound on the left and/or rear side of the President's skull [50, p. 174], nor were there any bullet fragments recovered from such a shot [38]; this rules out a high-speed, full-metal jacketed round, as such rounds would pass through the target. But additionally, it must be recalled that the “forward snap” observed at Z313 is unequivocally the result of a shot from the rear (as painstakingly demonstrated in §2.1), and this occurs *before* the rearward lurch. Thus, even if one allows the possibility of a shot from the front, it must be conceded that *any such hypothetical shot was, without question, first preceded by a shot from the rear.* The implication of this proposition is that the

shot from the front would then have entered an already-shattered skull¹⁰ as observed in Z313. It should now be clear to the reader that, from Eq. (2), it is precisely the collision and drag forces acting upon a projectile that impart an impulse force and acceleration on the target (indeed, this is how momentum is conserved), and these forces are directly proportional to projectile's presented area, A . Thus, a hypothetical full-metal jacketed round entering a shattered skull from the front would *not* impart a detectable impulse¹¹—it would simply pass through with little change in momentum, much like the shot that wounded the President in the lower neck.

But what about hollow-point, soft-point or frangible bullets? Again, the short answer would be “no” given that such fragments were never seen nor recovered [13, 38], as conservation of mass would require. But furthermore, from the wound ballistics perspective of this paper, it must be noted that there was *not* an observed second explosion of the head in Z314 or beyond, this being the attendant indicator of deformation (or “heating”) in brain tissue arising from a large loss in KE (Figure 4c) associated with the increased drag of a deformed bullet. For this reason, one may *also* rule out deforming bullets, as these are designed precisely for causing maximum energy transfer and damage to the target¹² [14]. And given the observed expulsion of mass in Z313–Z316 (Figure 5), conservation of momentum in the form of Eq. (27) *already predicts* a rearward recoil of the head cavity (of the same general magnitudes as that observed) in the absence of any frontal impulse.

3. Discussion and conclusions

This paper has presented a unique quantitative scientific analysis of gunshot wound dynamics observed in the Zapruder Film of the Kennedy Assassination. Based on known parameters of the crime scene, theoretical model calculations were performed for an idealized high-energy spherical projectile possessing the mass and speed (assuming air resistance over the 81 m distance between the muzzle and target; cf. Figure 1 and 2.1.2) of a Carcano military rifle bullet. The model projectile collides with and passes through a target that takes into account the cumulative

¹⁰ This was a hypothesis proposed by Dr. Cyril Wecht [4, 16, 50], a generally well-respected forensic pathologist who served on the HSCA.

¹¹ The author repeated impulse calculations for a “near-simultaneous shot” from the front assuming a full-metal jacketed round entering through the head wound. Summarizing, assuming an impact speed of 65,800 cm/s (the Carcano muzzle speed *without* air resistance), the estimated exit speed would be $\approx 57,000$ cm/s, and the estimated head snap ΔX brought on by the impulse forces would be 0.4 in per Zapruder Frame; thus it would take a full 5–6 Zapruder Frames simply to stop the observed 2.2–2.3 inch (≈ 6 cm) forward “head snap” occurring within a fraction of 1 frame between Z312–Z313, with no retrograde motion whatsoever.

¹² Anatomical modeling [15] reenactments of the Dallas crime-scene presented in the 2008 Discovery Channel program “JFK: Inside the Target Car” show a “complete obliteration” of the target (i.e., extreme damage to the test dummy head, far exceeding that observed in Dallas) resulting from a high-powered hollow-point round.

resistances presented by skull (cortical bone) and soft tissue (brain). The projectile deforms during target passage (initiated by the rigid skull collision), then deposits the majority of its KE to the target, a part of which is consumed toward imparting an instantaneous *impulse force* that propels the target forward by ≈ 2 inches (≈ 5 cm) during the course of one shutter cycle (i.e., with a speed of $\approx +2$ in/frame), the exact magnitude depending upon uncertainties in parameters such as the projectile deformation and impact time. The remainder of the KE goes toward “heating” (i.e., deforming and disrupting) the target soft tissue. The actual transfer of energy is known to occur through *temporary cavitation*, which increases the interaction region via a separated flow field, outward propagating pressure wave and restoring force undulations. In the Zapruder Film, the skull is observed to rupture (as a result of the temporary cavitation pressure) with a significant quantity of mass being propelled forward and upward from a single large opening on the mid-front right of the President’s head. The observed wound location roughly lags the computed location of maximum KE transfer, and a theoretical explosive “jet” exhaust speed was found to be of the same magnitude as that observed in the film. The delayed *observed forward momentum* of this jet (or spray) of material, occurring well after the projectile had passed, was then quantitatively shown to be associated with a short-lived *recoil effect* that imparted a backward change in velocity (i.e., deceleration) on the President’s head from the initial $\approx +2$ in/frame forward head snap to ≈ 0 to -3 in/frame (≈ 0 to -8 cm/frame) over the following shutter cycle (again depending upon uncertainties in parameters). Finally, it was shown that a second delayed backward acceleration (delayed relative to the impulse and recoil, but still rapid by everyday experience) is detectable in data published previously by [9], and this acceleration occurs on the President’s entire upper body (not just his head). The most plausible forcing mechanism for this second distinct backward acceleration (i.e., one that would act on the body’s CM and is consistent with the observed time scale) would be a nervous system reaction to massive brain injury as proposed by earlier investigators [50]. This *neuromuscular effect* causes the large torso muscles to undergo a delayed involuntary contraction, straightening the torso and thus torquing the entire upper body backward from its seated posture. From the foregoing modeling calculations and observations of the Zapruder Film it was thus quantitatively shown that the President’s reactions just after the projectile impact were physically consistent with a gunshot wound caused by a high-energy Carcano military rifle bullet fired from the vicinity of the TSBD.

In criminal homicide cases, establishment of facts is critical to establish causes, reconstruct the crime and properly assign guilt (or innocence). In the case of the “Crime of the Twentieth Century,” such a task is obviously of even greater importance given the historical dimension and relevance. Noted homicide prosecutor and Kennedy assassination expert Vincent Bugliosi had suggested that the conclusions of the WC would be wholly deducible had the Zapruder Film never

existed (i.e., from the autopsy and other forensic evidence), and thus he cautioned his readers not to make too much out of it [4, pp. 450–451, 464–466]. While he may indeed have been correct that the film was not necessary to solve the crime (and get a guilty verdict), it nevertheless is the case that the film provides remotely sensed optical data amenable to gunshot wound ballistic analysis. Although the “large-defect” wound location and forward expulsion of mass seen in Z313 are suggestive of a through-and-through trajectory from the rear, the recoil and neuromuscular effects in and of themselves do not identify the origin of the shot—the recoil was the result of the observed explosion in the wake of the projectile and the neuromuscular reaction could occur from any brain injury of that magnitude regardless of the projectile’s origin. However, these are indirect effects of the projectile-target interaction that quantitatively explain the *delayed* “back and to the left” motion observed in the Zapruder Film. On the other hand, the implications of the *instantaneous* impulse brought on by the high-speed projectile collision and passage through the target may be logically summarized as follows. If \mathcal{P} denotes “collision impulse in $\pm x$ direction” (i.e., cause) and \mathcal{Q} denotes “instantaneous change in target momentum in $\pm x$ direction” (i.e., effect), where the “target” here is President Kennedy’s head, then from physical reasoning the following logical statement holds

$$\mathcal{P} \Rightarrow \mathcal{Q}. \quad (33)$$

\mathcal{Q} is observed to be true in the Zapruder Film for the $+x$ (left to right down Elm Street) direction, which is consistent with statement (33) for the observed forward impulse. But if an equivalent statement is attempted for the hypothetical case occurring in the opposite $-x$ direction (i.e., originating from a shot to the front of the limousine), from the Zapruder Film \mathcal{Q} is false for reasons explained in Section 2.2. Thus, from the tautological expression

$$(\mathcal{P} \Rightarrow \mathcal{Q}) \Leftrightarrow (\neg \mathcal{Q} \Rightarrow \neg \mathcal{P}), \quad (34)$$

a frontal impact at Z313 is physically ruled out. Of course, the validity of statement (34) does not rule out conjectured *missed* shots (although no physical evidence was ever recovered for any such shots), nor does it pinpoint the exact origin of the shot that hit (e.g., the TSBD as opposed to another nearby building). But the modeling study (and underlying dynamics and conservation laws) presented in this paper, in corroboration of the autopsy findings [25], *do* imply that President Kennedy was *not hit* by a hypothesized gunshot from the front. The conclusion is an important one given that the hypothesized existence of a shooter in front of the limousine (viz., on the Grassy Knoll) has been the primary physical foundation for virtually all conspiracy conjectures to date on the topic.¹³ As a parting note, while the simple one-

¹³ It is recognized, however, that the physical implications of this paper do not rule out the *possibility* of a conspiracy, either in the form of (1) active participants firing and missing (e.g., as proposed by the HSCA), or, more plausibly (and perniciously), (2) like-minded associates *indirectly* aiding and abetting the assassin.

dimensional physical models presented in this paper were derived for application to a special case study (viz., the Kennedy Assassination), the underlying physical principles provide an approximate quantitative description of the interaction between a high-speed projectile (slowed by an intervening atmosphere) and a heterogenous body comprised of bone and visco-elastic tissue (viz., the human head), and may also form a basic conceptual basis for understanding the wounding mechanisms involved in such interactions.

Declarations

Author contribution statement

N. R. Nalli: Conceived and designed the experiments; Performed the experiments; Analyzed and interpreted the data; Contributed reagents, materials, analysis tools or data; Wrote the paper.

Funding statement

This research did not receive any specific grant from funding agencies in the public, commercial, or not-for-profit sectors.

Competing interest statement

The authors declare no conflict of interest.

Additional information

No additional information is available for this paper.

Acknowledgements

The following individuals and institutions are acknowledged for their support in the preparation of this work. First and foremost, I am grateful to Larry M. Sturdivan (wound ballistics expert for the HSCA) for very helpful discussions pertaining to his previous work as well as for reviewing my initial drafts and providing expert feedback. Krishna Shenoy, Mark Davies, and The Sixth Floor Museum at Dealey Plaza graciously provided ongoing research assistance as well as access to the digital high-resolution Zapruder frames used in the paper. Staff at the National Archives II, College Park, Maryland were very helpful in finding Warren

Commission documents, especially Gene Morris, the JFK Collection specialist. Jan Thomas (NOAA Betty Petersen Library) is acknowledged for his invaluable assistance with numerous reference books and specialized scientific journal paper requests cited in the bibliography. Vance Hum (IMSG President, CEO, and forensic scientist) and Hui Xu (IMSG Program Manager) are acknowledged for IMSG support, and Dr. Hum is additionally acknowledged for his review of the initial draft. John McAdams is recognized for maintaining a valuable internet resource and graciously responded to my inquires. I am also grateful for the critical reading and constructive professional feedback of the three anonymous peer-reviewers. Finally, this academic pursuit would not have been possible without the consistent support of my wife Christine, who also provided U.S. military expertise on firearms and assisted me on site visits to Dealey Plaza in Dallas. Accurate three-dimensional map rendering of Dealey Plaza in Figure 1 was made possible via Google Earth Pro.

References

- [1] D.R. Wrone, *The Zapruder Film: Reframing JFK's Assassination*, 2013th edition, University Press of Kansas, Lawrence, KS, 2003.
- [2] *Warren Commission Hearings, Hearings Before the President's Commission on the Assassination of President Kennedy*, vol. VII, 1964.
- [3] *Warren Commission Report, Report of the President's Commission on the Assassination of President Kennedy*, 1964.
- [4] V. Bugliosi, *Reclaiming History: The Assassination of President John F. Kennedy*, 1st edition, W. W. Norton & Company, Inc., New York, NY, 2007.
- [5] M. Ayton, D. Von Pein, *Beyond Reasonable Doubt: The Warren Report and Lee Harvey Oswald's Guilt and Motive 50 Years on*, Strategic Media Books, LLC, Rock Hill, SC, 2014.
- [6] G. Posner, *Case Closed: Lee Harvey Oswald and the Assassination of JFK*, first Anchor Books edition, Anchor Books, New York, NY, 1993.
- [7] D.B. Thomas, *Hear No Evil: Politics, Science & the Forensic Evidence in the Kennedy Assassination*, Skyhorse Publishing, New York, NY, 2010.
- [8] M. Lane, *Rush to Judgement: A Critique of the Warren Commission's Inquiry Into the Murders of President John F. Kennedy, Officer J. D. Tippit and Lee Harvey Oswald*, The Lane Group, LLC, 2013, first edition, The Lane Group, LLC, Charlottesville, VA, 1966.
- [9] J. Thompson, *Six Seconds in Dallas: A Micro-Study of the Kennedy Assassination*, Bernard Geis Associates, Random House, New York, NY, 1967.

- [10] L.W. Alvarez, A physicist examines the Kennedy assassination film, *Am. J. Phys.* 44 (9) (1976) 813–827.
- [11] J.K. Lattimer, E.B. Schlesinger, H.H. Merritt, President Kennedy's spine hit by first bullet, *Bull. N. Y. Acad. Med.* 53 (3) (1977) 280–291.
- [12] J.K. Lattimer, J.K. Lattimer, G. Lattimer, E. Haubner, A. Laidlaw, V. Forgett, Differences in the wounding behavior of the two bullets that struck President Kennedy; an experimental study, *Wound Ballist. Rev.* 2 (2) (1996) 13–37.
- [13] L.C. Haag, President Kennedy's fatal head wound and his rearward head snap, *AFTE J.* 46 (4) (2014) 279–289.
- [14] P.K. Stefanopoulos, G.F. Hadjigeorgiou, K. Filippakis, D. Gyftokostas, Gunshot wounds: a review of ballistics related to penetrating trauma, *J. Acute Dis.* 3 (3) (2014) 178–185.
- [15] C. Humphrey, J. Kumaratilake, Ballistics and anatomical modelling—a review, *Leg. Med.* 23 (2016) 21–29.
- [16] L.M. Sturdivan, *The JFK Myths: A Scientific Investigation of the Kennedy Assassination*, 1st edition, Paragon House, St. Paul, MN, 2005.
- [17] F.S. DeRonja, M. Holland, A technical investigation pertaining to the first shot fired in the JFK assassination, *J. Assoc. Crime Scene Reconstr.* 20 (2016) 9–33.
- [18] E. Courtney, A. Courtney, L. Andrusiv, M. Courtney, Experimental studies of terminal performance of lead-free pistol bullets in ballistic gelatin using high speed video, *Investig. Sci. J.* 9 (1) (2017) 1–18.
- [19] V.D. Barger, M.G. Olsson, *Classical Mechanics: A Modern Perspective*, 2nd edition, McGraw-Hill, Inc., New York, NY, 1995.
- [20] L.M. Sturdivan, R. Bexon, A Mathematical Model of the Probability of Perforation of the Human Skull by a Ballistic Projectile, Tech. Rep. ARCSL-TR-81001, Chemical Systems Laboratory, Aberdeen Proving Ground, Maryland, April 1981.
- [21] HSCA, *Investigation of the Assassination of President John F. Kennedy*, Appendix to Hearings, vol. VI, Photographic Evidence, 1979.
- [22] P.A. Finck, Ballistic and forensic pathologic aspects of missile wounds. Conversion between Anglo-American and metric-system units, *Mil. Med.* 130 (5) (1965) 545–569.
- [23] J. Peterson, P.C. Dechow, Material properties of the inner and outer cortical tables of the human parietal bone, *Anat. Rec.* 268 (2002) 7–15.

- [24] M. Cammarata, F. Nicoletti, M.D. Paola, A. Valenza, G. Zummo, Mechanical behavior of human bones with different saturation levels, in: Conference: 2nd International Electronic Conference on Materials, 2016.
- [25] D.L. Breo, JFK's death—the plain truth from the MDs who did the autopsy, *JAMA* 267 (20) (1992) 2794–2803, at Large With Dennis L. Breo.
- [26] E.J. Routh, *The Elementary Part of a Treatise on the Dynamics of a System of Rigid Bodies*, seventh revised and enlarged edition, The MacMillan Company, New York, NY, 1905.
- [27] R.O. Ritchie, M.J. Buehler, P. Hansma, Plasticity and toughness in bone, *Phys. Today* 62 (6) (2009) 41–47.
- [28] J. Wendlova, Bone quality: elasticity and strength, *Bratisl. Lek. Listy* 109 (9) (2008) 383–386.
- [29] J.H. McElhaney, J.L. Fogle, J.W. Melvin, R.R. Haynes, V.L. Roberts, N.M. Alem, Mechanical properties of cranial bone, *J. Biomech.* 3 (1970) 495–511.
- [30] H. Halliday, R. Resnick, J. Walker, *Fundamentals of Physics*, 5th edition, John Wiley & Sons, Inc., New York, NY, 1997.
- [31] T.M. Keaveny, E.F. Morgan, O.C. Yeh, Bone mechanics, Ch. 8, in: *Standard Handbook of Biomedical Engineering & Design*, McGraw-Hill, New York, NY, 2004, pp. 8.1–8.23, downloaded from Digital Engineering Library, www.digitalengineeringlibrary.com.
- [32] C.D. Hodgman (Ed.), *CRC Standard Mathematical Tables*, twelfth edition, Chemical Rubber Publishing Company, Cleveland, OH, 2005.
- [33] L.M. Sturdivan, *A Mathematical Model for Assessing Weapons Effects from Gelatin Penetration by Spheres*, Tech. Rep. EB-TR-73022, Edgewood Arsenal, Aberdeen Proving Ground, Maryland, September 1973.
- [34] C.E. Peters, A mathematical-physical model of wound ballistics, *J. Trauma (China)* 6 (2) (1990) 303–318, supplement.
- [35] L.M. Sturdivan, *A Mathematical Model of Penetration of Chunky Projectiles in a Gelatin Tissue Simulant*, Tech. Rep. ARCSL-TR-78055, Chemical Systems Laboratory, Aberdeen Proving Ground, Maryland, August 1978.
- [36] J.M. Ryan, G.J. Cooper, R.L. Maynard, Wound ballistics: contemporary and future research, *J. R. Army Med. Corps* 134 (1988) 119–125.
- [37] J.J. Hollerman, M.L. Fackler, D.M. Coldwell, Y. Ben-Menachem, Gunshot wounds: 1. Bullets, ballistics, and mechanisms of injury, *AJR* 155 (1990) 685–690.

- [38] L.C. Haag, President Kennedy's fatal gunshot wound and the seemingly anomalous behavior of the fatal bullet, *AFTE J.* 46 (3) (2014) 218–223.
- [39] A.B. Bailey, J. Hiatt, Sphere drag coefficients for a broad range of Mach and Reynolds numbers, *AIAA J.* 10 (11) (1972) 1436–1440.
- [40] E. Courtney, A. Courtney, M. Courtney, Experimental Tests of the Proportionality of Aerodynamic Drag to Air Density for Supersonic Projectiles, Cornell University Library, 2015, pp. 1–8, arXiv:1510.07336.
- [41] A.G. Olivier, A.J. Dziemian, Wound Ballistics of 6.5-mm Mannlicher-Carcano Ammunition (U), Tech. Rep. CRDLR 3264, US Army Edgewood Arsenal, Chemical Research and Development Laboratories, Edgewood, Maryland, March 1965.
- [42] J.M. Wallace, P.V. Hobbs, Atmospheric Science: An Introductory Survey, Academic Press, San Diego, California, 1977.
- [43] R.B. Stull, An Introduction to Boundary Layer Meteorology, Kluwer Academic Publishers, Dordrecht, The Netherlands, 1988.
- [44] R.W. Hyland, A. Wexler, Formulations for the thermodynamic properties of the saturated phases of H₂O from 173.15 K to 473.15 K, *ASHRAE Trans.* 2A (1983) 500–519.
- [45] NOAA/NESDIS National Climatic Data Center (NCDC), Global Surface Hourly database, <https://www7.ncdc.noaa.gov/CDO/cdopomain.cmd>.
- [46] N. Yoganandan, F.A. Pintar, J. Zhang, J.L. Baisden, Physical properties of the human head: mass, center of gravity and moment of inertia, *J. Biomech.* 42 (2009) 1177–1192.
- [47] T.W. Barber, J.A. Brockway, L.S. Higgins, The density of tissues in and about the head, *Acta Neurol. Scand.* 46 (1970) 85–92.
- [48] J.R. Taylor, An Introduction to Error Analysis: The Study of Uncertainties in Physical Measurements, 2nd edition, University Science Books, Sausalito, CA, 1997.
- [49] A. Courtney, M. Courtney, Physical Mechanisms of Soft Tissue Injury from Penetrating Ballistic Impact, Tech. rep., DFRL, U.S. Air Force Academy, Colorado, November 2012.
- [50] HSCA, Investigation of the Assassination of President John F. Kennedy, Appendix to Hearings, vol. VII, Medical and Firearms Evidence, 1979.
- [51] L. Wolpert, The Unnatural Nature of Science, second printing edition, Harvard University Press, Cambridge, MA, 1994.

- [52] Itek Corporation, John Kennedy Assassination Film Analysis, Report 180-10001-10396, Select Committee on Assassinations, U.S. House of Representatives, U.S. Government Printing Office, Washington, D.C., May 1976.
- [53] J.B. Marion, S.T. Thornton, Classical Dynamics of Particles and Systems, 4th edition, Harcourt Brace College Publishers, Fort Worth, TX, 1995.
- [54] C.C. Henery, T.M. Mayhew, The cerebrum and cerebellum of the fixed human brain: efficient and unbiased estimates of volumes and cortical surface areas, *J. Anat.* 167 (1989) 167–180.
- [55] G. Joos, Theoretical Physics, 2nd edition, Hafner Publishing Company, New York, NY, 1950, 853 pp.
- [56] D.S. Lifton, Best Evidence: Disguise and Deception in the Assassination of John F. Kennedy, First Carroll & Graf, twelfth printing edition, Carroll & Graf Publishers, Inc., New York, NY, 1980, 1992.
- [57] G.P. Chambers, Head Shot: The Science Behind the JFK Assassination, expanded edition, Prometheus Books, Amherst, NY, 2012.
- [58] G.L. Aguilar, C. Wecht, Letter to the editor: tracking the ‘magic’ bullet in the JFK assassination. . . , *AFTE J.* 47 (3) (2015) 131–138.